

Electroweak Theory

Wolfgang Hollik

Max-Planck-Institut für Physik (Werner-Heisenberg-Institut),
Föhringer Ring 6, D-80805 Munich, Germany

E-mail: hollik@mppmu.mpg.de

Abstract. In this lecture we discuss the electroweak Standard Model, its quantum effects, and precision tests. We give an introduction to the construction of the basic Lagrangian, some details on the calculation of amplitudes at the one-loop level, higher-order calculations for electroweak precision observables are obtained, with emphasis on the W , Z masses and the Z resonance observables. The predictions of the Standard Model are compared with the experimental data, with implications for the Higgs bosons. A brief look to the supersymmetric extension of the Standard Model in terms of the MSSM and its performance in view of the precision data concludes the lecture.

1. Introduction

The electroweak Standard Model [1-3] is the commonly accepted theory of the fundamental electroweak interaction. It is a gauge invariant quantum field theory based on the symmetry group $SU(2) \times U(1)$, which is spontaneously broken by the Higgs mechanism. The renormalizability of the Standard Model [4] allows us to make precise predictions for measurable quantities also in higher orders of the perturbative expansion, in terms of a few input parameters. The higher-order terms, radiative corrections or quantum corrections, contain the self-coupling of the vector bosons as well as their interactions with the Higgs field and the top quark, even for processes involving only light fermions. Their calculation provides the theoretical basis for electroweak precision tests. Assuming the validity of the Standard model, the presence of the top quark and the Higgs boson in the loop contributions to electroweak observables allows us to obtain indirectly significant bounds on their masses from precision measurements of these observables. The only unknown quantity at present is the Higgs boson. Its mass is nowadays getting more and more constrained, by a comparison of the Standard Model predictions with the experimental data.

The high precision experiments impose stringent tests on the Standard Model. The experimental accuracy in the electroweak observables has reached the level of the quantum effects, and requires the highest standards on the theoretical side as well. A sizeable amount of work has continuously contributed over the last two decades to a steadily rising improvement of the standard model predictions, pinning down the theoretical uncertainties to the level required for the proper interpretation of the precision data. Also for the minimal supersymmetric standard model (MSSM), remarkable progress has to be reported in predicting the precision observables with similar accuracy as in the standard model.

In these lectures we give a brief discussion of the structure of the Standard Model and its quantum corrections for testing the electroweak theory at present and future colliders. The

predictions for the vector boson masses, cross sections, and the Z resonance observables like the width of the Z resonance, partial widths, effective neutral current coupling constants and mixing angles at the Z peak, and address the study of the vector-boson self-interaction. Comparisons with the recent experimental data are shown and their implications for the Higgs sector are discussed. Giving an outlook, as a successful example of physics beyond the Standard Model the MSSM is briefly discussed in the light of precision data.

2. Formulation of the Standard Model

2.1. The classical Lagrangian

The fundamental fermions, as families with left-handed doublets and right-handed singlets, appear as the fundamental representation of the group $SU(2) \times U(1)$,

$$\begin{pmatrix} \nu_e \\ e \end{pmatrix}_L, \quad \begin{pmatrix} \nu_\mu \\ \mu \end{pmatrix}_L, \quad \begin{pmatrix} \nu_\tau \\ \tau \end{pmatrix}_L, \quad e_R, \quad \mu_R, \quad \tau_R$$

$$\begin{pmatrix} u \\ d \end{pmatrix}_L, \quad \begin{pmatrix} c \\ s \end{pmatrix}_L, \quad \begin{pmatrix} t \\ b \end{pmatrix}_L, \quad u_R, \quad d_R, \quad c_R, \dots$$

They can be classified by the quantum numbers of the weak isospin I , I_3 , and the weak hypercharge Y . The Gell-Mann–Nishijima relation establishes the relation of these basic quantum numbers to the electric charge Q :

$$Q = I_3 + \frac{Y}{2}. \quad (1)$$

This structure can be incorporated in a gauge invariant field theory of the unified electromagnetic and weak interactions by interpreting $SU(2) \times U(1)$ as the group of gauge transformations under which the Lagrangian is invariant. This full symmetry has to be broken by the Higgs mechanism down to the electromagnetic gauge symmetry; otherwise the W^\pm , Z bosons would be massless. The minimal formulation, the Standard Model, requires a single Higgs field which is a doublet under $SU(2)$.

According to the general principles of constructing a gauge invariant field theory with spontaneous symmetry breaking, the gauge, Higgs, and fermion parts of the electroweak Lagrangian

$$\mathcal{L}_{cl} = \mathcal{L}_G + \mathcal{L}_H + \mathcal{L}_F \quad (2)$$

are specified in the following way:

Gauge fields. $SU(2) \times U(1)$ is a non-Abelian group which is generated by the isospin operators I_1 , I_2 , I_3 and the hypercharge Y (the elements of the corresponding Lie algebra). Each of these generalized charges is associated with a vector field: a triplet of vector fields $W_\mu^{1,2,3}$ with $I_{1,2,3}$ and a singlet field B_μ with Y . The isotriplet W_μ^a , $a = 1, 2, 3$, and the isosinglet B_μ lead to the field strength tensors

$$W_{\mu\nu}^a = \partial_\mu W_\nu^a - \partial_\nu W_\mu^a + g_2 \epsilon_{abc} W_\mu^b W_\nu^c,$$

$$B_{\mu\nu} = \partial_\mu B_\nu - \partial_\nu B_\mu. \quad (3)$$

g_2 denotes the non-Abelian $SU(2)$ gauge coupling constant and g_1 the Abelian $U(1)$ coupling. From the field tensors (3) the pure gauge field Lagrangian

$$\mathcal{L}_G = -\frac{1}{4} W_{\mu\nu}^a W^{\mu\nu,a} - \frac{1}{4} B_{\mu\nu} B^{\mu\nu} \quad (4)$$

is formed, which is invariant under non-Abelian gauge transformations.

Fermion fields and fermion–gauge interactions. The left-handed fermion fields of each lepton and quark family

$$\psi_j^L = \begin{pmatrix} \psi_{j+}^L \\ \psi_{j-}^L \end{pmatrix}$$

with family index j are grouped into $SU(2)$ doublets with component index $\sigma = \pm$, and the right-handed fields into singlets

$$\psi_j^R = \psi_{j\sigma}^R.$$

Each left- and right-handed multiplet is an eigenstate of the weak hypercharge Y such that the relation (1) is fulfilled. The covariant derivative

$$D_\mu = \partial_\mu - i g_2 I_a W_\mu^a + i g_1 \frac{Y}{2} B_\mu \quad (5)$$

induces the fermion–gauge field interaction via the minimal substitution rule

$$\mathcal{L}_F = \sum_j \bar{\psi}_j^L i \gamma^\mu D_\mu \psi_j^L + \sum_{j,\sigma} \bar{\psi}_{j\sigma}^R i \gamma^\mu D_\mu \psi_{j\sigma}^R. \quad (6)$$

Higgs field and Higgs interactions. For spontaneous breaking of the $SU(2) \times U(1)$ symmetry leaving the electromagnetic gauge subgroup $U(1)_{em}$ unbroken, a single complex scalar doublet field with hypercharge $Y = 1$

$$\Phi(x) = \begin{pmatrix} \phi^+(x) \\ \phi^0(x) \end{pmatrix} \quad (7)$$

is coupled to the gauge fields through

$$\mathcal{L}_H = (D_\mu \Phi)^+ (D^\mu \Phi) - V(\Phi) \quad (8)$$

with the covariant derivative

$$D_\mu = \partial_\mu - i g_2 I_a W_\mu^a + i \frac{g_1}{2} B_\mu.$$

The Higgs field self-interaction

$$V(\Phi) = -\mu^2 \Phi^+ \Phi + \frac{\lambda}{4} (\Phi^+ \Phi)^2 \quad (9)$$

is constructed in such a way that Φ has a non-vanishing vacuum expectation value

$$\langle \Phi \rangle = \frac{1}{\sqrt{2}} \begin{pmatrix} 0 \\ v \end{pmatrix} \quad \text{with} \quad v = \frac{2\mu}{\sqrt{\lambda}}. \quad (10)$$

The field (7) can be written in the following way:

$$\Phi(x) = \begin{pmatrix} \phi^+(x) \\ (v + H(x) + i\chi(x))/\sqrt{2} \end{pmatrix}, \quad (11)$$

where the components ϕ^+ , H , χ have vacuum expectation values zero. Exploiting the invariance of the Lagrangian, the components ϕ^+ , χ can be gauged away; this means that they are unphysical (Higgs ghosts or would-be Goldstone bosons). In this particular gauge, the unitary gauge, the Higgs field has the simple form

$$\Phi(x) = \frac{1}{\sqrt{2}} \begin{pmatrix} 0 \\ v + H(x) \end{pmatrix}.$$

The real field $H(x)$ describes physical neutral scalar particles with mass

$$M_H = \mu\sqrt{2}. \quad (12)$$

The Higgs field components have triple and quartic self couplings following from V , and couplings to the gauge fields via the kinetic term of Eq. (8).

In addition, Yukawa couplings to fermions are introduced in order to make the charged fermions massive. The Yukawa term is conveniently expressed in the doublet field components (7), for one family of leptons and quarks given by (ϕ^- denotes the adjoint of ϕ^+)

$$\begin{aligned} \mathcal{L}_{Yukawa} &= -g_l (\bar{\nu}_L \phi^+ l_R + \bar{l}_R \phi^- \nu_L + \bar{l}_L \phi^0 l_R + \bar{l}_R \phi^{0*} l_L) \\ &= -g_d (\bar{u}_L \phi^+ d_R + \bar{d}_R \phi^- u_L + \bar{d}_L \phi^0 d_R + \bar{d}_R \phi^{0*} d_L) \\ &\quad - g_u (-\bar{u}_R \phi^+ d_L - \bar{d}_L \phi^- u_R + \bar{u}_R \phi^0 u_L + \bar{u}_L \phi^{0*} u_R). \end{aligned} \quad (13)$$

The fermion mass terms follow from the v -part of ϕ^0 . The Yukawa coupling constants $g_{l,d,u}$ are related to the masses of the charged fermions by

$$m_f = g_f \frac{v}{\sqrt{2}} = \sqrt{2} \frac{g_f}{g_2} M_W. \quad (14)$$

In the unitary gauge the Yukawa Lagrangian is particularly simple:

$$\mathcal{L}_{Yukawa} = - \sum_f m_f \bar{\psi}_f \psi_f - \sum_f \frac{m_f}{v} \bar{\psi}_f \psi_f H. \quad (15)$$

As a remnant of this mechanism, Yukawa interactions between the massive fermions and the physical Higgs field occur with coupling constants proportional to the fermion masses.

Physical fields and parameters. The gauge invariant Higgs–gauge field interaction in the kinetic part of Eq. (8) gives rise to mass terms for the vector bosons in the non-diagonal form

$$\frac{1}{2} \left(\frac{g_2}{2} v \right)^2 (W_1^2 + W_2^2) + \frac{v^2}{4} (W_\mu^3, B_\mu) \begin{pmatrix} g_2^2 & g_1 g_2 \\ g_1 g_2 & g_1^2 \end{pmatrix} \begin{pmatrix} W_\mu^3 \\ B_\mu \end{pmatrix}. \quad (16)$$

The physical content becomes transparent by performing a transformation from the fields W_μ^a , B_μ (in terms of which the symmetry is manifest) to the physical fields

$$W_\mu^\pm = \frac{1}{\sqrt{2}} (W_\mu^1 \mp i W_\mu^2) \quad (17)$$

and

$$\begin{pmatrix} Z_\mu \\ A_\mu \end{pmatrix} = \begin{pmatrix} \cos \theta_W & \sin \theta_W \\ -\sin \theta_W & \cos \theta_W \end{pmatrix} \begin{pmatrix} W_\mu^3 \\ B_\mu \end{pmatrix}. \quad (18)$$

In these fields the mass term (16) is diagonal and has the form

$$M_W^2 W_\mu^+ W_\mu^- + \frac{1}{2} (A_\mu, Z_\mu) \begin{pmatrix} 0 & 0 \\ 0 & M_Z^2 \end{pmatrix} \begin{pmatrix} A^\mu \\ Z^\mu \end{pmatrix} \quad (19)$$

with

$$\begin{aligned} M_W &= \frac{1}{2} g_2 v, \\ M_Z &= \frac{1}{2} \sqrt{g_1^2 + g_2^2} v. \end{aligned} \quad (20)$$

The mixing angle in the rotation (18) is given by

$$\cos \theta_W = \frac{g_2}{\sqrt{g_1^2 + g_2^2}} = \frac{M_W}{M_Z}. \quad (21)$$

Identifying A_μ with the photon field which couples via the electric charge $e = \sqrt{4\pi\alpha}$ to the electron, e can be expressed in terms of the gauge couplings in the following way,

$$e = \frac{g_1 g_2}{\sqrt{g_1^2 + g_2^2}}, \quad \text{or} \quad g_2 = \frac{e}{\sin \theta_W}, \quad g_1 = \frac{e}{\cos \theta_W}. \quad (22)$$

The relations above allow us to replace the original set of parameters $g_2, g_1, \lambda, \mu^2, g_f$ by the equivalent set of more physical parameters e, M_W, M_Z, M_H, m_f where each of them can (in principle) directly be measured in a suitable experiment.

An additional very precisely measured parameter is the Fermi constant G_μ , which is the effective 4-fermion coupling constant in the the Fermi model, measured via the muon lifetime (see section 4.1),

$$G_\mu = 1.16637(1) \cdot 10^{-5} \text{ GeV}^{-2}. \quad (23)$$

Consistency of the Standard Model at $q^2 \ll M_W^2$ with the Fermi model requires the identification

$$\frac{G_\mu}{\sqrt{2}} = \frac{e^2}{8 \sin^2 \theta_W M_W^2}, \quad (24)$$

which allows us to relate the vector boson masses to the parameters α, G_μ , and $\sin^2 \theta_W$ as follows,

$$\begin{aligned} M_W^2 &= \frac{\pi \alpha}{\sqrt{2} G_\mu} \cdot \frac{1}{\sin^2 \theta_W} \\ M_Z^2 &= \frac{\pi \alpha}{\sqrt{2} G_\mu} \cdot \frac{1}{\sin^2 \theta_W \cos^2 \theta_W}, \end{aligned} \quad (25)$$

and thus to establish also the M_W - M_Z interdependence:

$$M_W^2 \left(1 - \frac{M_W^2}{M_Z^2} \right) = \frac{\pi \alpha}{\sqrt{2} G_\mu}. \quad (26)$$

2.2. Quantization

Since the S -matrix element for any physical process is a gauge-invariant quantity, it is possible to work in the unitary gauge with no unphysical particles in internal lines. For a systematic treatment of the quantization of \mathcal{L}_{cl} and for higher order calculations, however, one better refers to a renormalizable gauge. This can be done by adding to \mathcal{L}_{cl} a gauge-fixing Lagrangian, for example

$$\mathcal{L}_{fix} = -\frac{1}{2} \left(F_\gamma^2 + F_Z^2 + 2F_+F_- \right) \quad (27)$$

with linear gauge fixings of the 't Hooft type:

$$\begin{aligned} F_\pm &= \frac{1}{\sqrt{\xi^W}} \left(\partial^\mu W_\mu^\pm \mp i M_W \xi^W \phi^\pm \right) \\ F_Z &= \frac{1}{\sqrt{\xi^Z}} \left(\partial^\mu Z_\mu - M_Z \xi^Z \chi \right) \\ F_\gamma &= \frac{1}{\sqrt{\xi^\gamma}} \partial^\mu A_\mu \end{aligned} \quad (28)$$

with arbitrary parameters $\xi^{W,Z,\gamma}$. In this class of 't Hooft gauges, the vector boson propagators have the form

$$\begin{aligned} \frac{i}{k^2 - M_V^2} \left(-g^{\mu\nu} + \frac{(1 - \xi^V) k^\mu k^\nu}{k^2 - \xi^V M_V^2} \right) = \\ \frac{i}{k^2 - M_V^2} \left(-g^{\mu\nu} + \frac{k^\mu k^\nu}{k^2} \right) + \frac{i \xi^V}{k^2 - \xi^V M_V^2} \frac{k^\mu k^\nu}{k^2}, \end{aligned} \quad (29)$$

and the propagators for the unphysical Higgs fields are given by

$$\begin{aligned} \frac{i}{k^2 - \xi^W M_W^2} &\quad \text{for } \phi^\pm \\ \frac{i}{k^2 - \xi^Z M_Z^2} &\quad \text{for } \chi^0. \end{aligned} \quad (30)$$

Higgs–vector boson transitions do not occur in the 't Hooft gauge.

For completion of the renormalizable Lagrangian, the Faddeev–Popov ghost term \mathcal{L}_{gh} has to be added [5] in order to balance the undesired effects in the unphysical components introduced by \mathcal{L}_{fix} :

$$\mathcal{L} = \mathcal{L}_{cl} + \mathcal{L}_{fix} + \mathcal{L}_{gh} \quad (31)$$

where

$$\mathcal{L}_{gh} = \bar{u}^\alpha(x) \frac{\delta F^\alpha}{\delta \theta^\beta(x)} u^\beta(x) \quad (32)$$

with ghost fields u^γ , u^Z , u^\pm , and $\frac{\delta F^\alpha}{\delta \theta^\beta}$ being the change of the gauge fixing operators (28) under infinitesimal gauge transformations characterized by $\theta^\alpha(x) = \{\theta^a(x), \theta^Y(x)\}$.

In the 't Hooft–Feynman gauge ($\xi = 1$) the vector boson propagators (29) become particularly simple: the transverse and longitudinal components, as well as the propagators for the unphysical Higgs fields ϕ^\pm , χ and the ghost fields u^\pm , u^Z , have poles which coincide with the masses of the corresponding physical particles W^\pm and Z .

2.3. Feynman rules for propagators and fermionic vertices

Expressed in terms of the physical parameters we can write down the Lagrangian

$$\mathcal{L}(A_\mu, W_\mu^\pm, Z_\mu, H, \phi^\pm, \chi, u^\pm, u^Z, u^\gamma; M_W, M_Z, e, \dots)$$

in a way which allows us to read off the propagators and the vertices most directly. In the $R_{\xi=1}$ gauge, the vector boson propagators have the particularly simple algebraic form $\sim g_{\mu\nu}$.

Fermion–gauge interactions:

$$\begin{aligned} J_{em}^\mu A_\mu : &\quad -i e Q_f \gamma_\mu \\ J_{NC}^\mu Z_\mu : &\quad i \frac{e}{2 \sin \theta_W \cos \theta_W} \gamma_\mu (v_f - a_f \gamma_5) \\ J_{CC}^\mu W_\mu : &\quad i \frac{e}{2\sqrt{2} \sin \theta_W} \gamma_\mu (1 - \gamma_5) V_{jk} \end{aligned} \quad (33)$$

Fermion–Higgs interactions:

$$- \frac{g_f}{\sqrt{2}} \bar{f} f H : \quad -i \frac{g_f}{\sqrt{2}} = i \frac{e}{2 \sin \theta_W} \frac{m_f}{M_W} \quad (34)$$

These Feynman rules provide the ingredients to calculate the lowest order amplitudes for fermionic processes. A complete list of all interaction vertices can be found e.g. in [10].

The processes of lepton and quark pair production at high-energy colliders are basically four-fermion processes. These are mediated by the gauge bosons (Higgs boson exchange can be neglected, owing to their small Yukawa couplings) and, sufficient to lowest order, defined by the vertices for the fermions interacting with the vector bosons. They are given in the Lagrangian above for the electromagnetic, neutral and charged current interactions. The neutral current coupling constants in (33) read

$$\begin{aligned} v_f &= I_3^f - 2Q_f \sin^2 \theta_W, \\ a_f &= I_3^f. \end{aligned} \quad (35)$$

Q_f and I_3^f denote the charge and the third isospin component of f_L . The quantities V_{jk} in the charged current vertex are the elements of the unitary CKM matrix

$$V_{\text{CKM}} = \begin{pmatrix} V_{ud} & V_{us} & V_{ub} \\ V_{cd} & V_{cs} & V_{cb} \\ V_{td} & V_{ts} & V_{tb} \end{pmatrix} \quad (36)$$

which describes family mixing in the quark sector [3]. Its origin is the diagonalization of the quark mass matrices from the Yukawa coupling which appears since quarks of the same charge have different masses. For massless neutrinos no mixing in the leptonic sector is present. Owing to the unitarity of V_{CKM} the mixing is absent in the neutral current.

3. Higher-order calculations

3.1. Dimensional regularization

In this section we provide some technical details for the calculation of radiative corrections for electroweak precision observables. The methods used are essentially based on the work of [6] and [7].

The diagrams with closed loops occurring in higher order perturbation theory involve integrals over the loop momentum. These integrals are in general divergent for large integration momenta (UV divergence). For this reason we need a regularization, which is a procedure to redefine the integrals in such a way that they become finite and mathematically well-defined objects. The widely used regularization procedure for gauge theories is that of dimensional regularization [8], which is Lorentz and gauge invariant: replace the dimension 4 by a lower dimension D where the integrals are convergent:

$$\int \frac{d^4 k}{(2\pi)^4} \rightarrow \mu^{4-D} \int \frac{d^D k}{(2\pi)^D} \quad (37)$$

An (arbitrary) mass parameter μ has been introduced in order to keep the dimensions of the coupling constants in front of the integrals independent of D . After renormalization the results for physical quantities are finite in the limit $D \rightarrow 4$.

The metric tensor in D dimensions has the property

$$g_\mu^\mu = g_{\mu\nu} g^{\nu\mu} = \text{Tr}(1) = D. \quad (38)$$

The Dirac algebra in D dimensions

$$\{\gamma_\mu, \gamma_\nu\} = 2 g_{\mu\nu} \mathbf{1} \quad (39)$$

has the consequences

$$\begin{aligned}
\gamma_\mu \gamma^\mu &= D \mathbf{1} \\
\gamma_\rho \gamma_\mu \gamma^\rho &= (2 - D) \gamma_\mu \\
\gamma_\rho \gamma_\mu \gamma_\nu \gamma^\rho &= 4g_{\mu\nu} \mathbf{1} - (4 - D) \gamma_\mu \gamma_\nu \\
\gamma_\rho \gamma_\mu \gamma_\nu \gamma_\sigma \gamma^\rho &= -2 \gamma_\sigma \gamma_\nu \gamma_\mu + (4 - D) \gamma_\mu \gamma_\nu \gamma_\sigma
\end{aligned} \tag{40}$$

A consistent treatment of γ_5 in D dimensions is more subtle [9]. However, in theories that are anomaly free, like the Standard Model, we can use γ_5 at the one-loop level as anticommuting with γ_μ ,

$$\{\gamma_\mu, \gamma_5\} = 0. \tag{41}$$

3.2. Example: One- and two-point integrals

In the calculation of self-energy diagrams the following types of one-loop integrals appear:

1-point integral:

$$\mu^{4-D} \int \frac{d^D k}{(2\pi)^D} \frac{1}{k^2 - m^2} =: \frac{i}{16\pi^2} A(m) \tag{42}$$

2-point integrals:

$$\begin{aligned}
\mu^{4-D} \int \frac{d^D k}{(2\pi)^D} \frac{1}{[k^2 - m_1^2][(k+q)^2 - m_2^2]} &=: \frac{i}{16\pi^2} B_0(q^2, m_1, m_2) \\
\mu^{4-D} \int \frac{d^D k}{(2\pi)^D} \frac{k_\mu; k_\mu k_\nu}{[k^2 - m_1^2][(k+q)^2 - m_2^2]} &=: \frac{i}{16\pi^2} B_{\mu; \mu\nu}(q^2, m_1, m_2).
\end{aligned} \tag{43}$$

The vector and tensor integrals B_μ , $B_{\mu\nu}$ can be expanded into Lorentz covariants and scalar coefficients,

$$\begin{aligned}
B_\mu &= q_\mu B_1(q^2, m_1, m_2) \\
B_{\mu\nu} &= g_{\mu\nu} B_{22}(q^2, m_1, m_2) + q_\mu q_\nu B_{21}(q^2, m_1, m_2).
\end{aligned} \tag{44}$$

The coefficient functions can be obtained algebraically from the scalar 1- and 2-point integrals A and B_0 , yielding

$$\begin{aligned}
B_1(q^2, m_1, m_2) &= \frac{1}{2q^2} \left[A(m_1) - A(m_2) + (m_1^2 - m_2^2 - q^2) B_0(q^2, m_1, m_2) \right] \\
B_{22}(q^2, m_1, m_2) &= \frac{1}{6} \left[A(m_2) + 2m_1^2 B_0(q^2, m_1, m_2) \right. \\
&\quad \left. + (q^2 + m_1^2 - m_2^2) B_1(q^2, m_1, m_2) + m_1^2 + m_2^2 - \frac{q^2}{3} \right] \\
B_{21}(q^2, m_1, m_2) &= \frac{1}{3q^2} \left[A(m_2) - m_1^2 B_0(q^2, m_1, m_2) \right. \\
&\quad \left. - 2(q^2 + m_1^2 - m_2^2) B_1(q^2, m_1, m_2) - \frac{m_1^2 + m_2^2}{2} + \frac{q^2}{6} \right].
\end{aligned} \tag{45}$$

Finally we have to calculate the scalar integrals A and B_0 . With help of the Feynman parametrization

$$\frac{1}{ab} = \int_0^1 dx \frac{1}{[ax + b(1-x)]^2}$$

and after a shift in the k -variable, B_0 can be written in the form

$$\begin{aligned} \frac{i}{16\pi^2} B_0(q^2, m_1, m_2) = & \\ \int_0^1 dx \frac{\mu^{4-D}}{(2\pi)^D} \int & \frac{d^D k}{[k^2 - x^2 q^2 + x(q^2 + m_1^2 - m_2^2) - m_1^2]^2}. \end{aligned} \quad (46)$$

The advantage of this parametrization is a simpler k -integration where the integrand is only a function of $k^2 = (k^0)^2 - \vec{k}^2$. In order to transform it into a Euclidean integral we perform the substitution ¹

$$k^0 = i k_E^0, \quad \vec{k} = \vec{k}_E, \quad d^D k = i d^D k_E$$

where the new integration momentum k_E has a definite metric:

$$k^2 = -k_E^2, \quad k_E^2 = (k_E^0)^2 + \dots + (k_E^{D-1})^2.$$

This leads us to a Euclidean integral over k_E :

$$\frac{i}{16\pi^2} B_0 = i \int_0^1 dx \frac{\mu^{4-D}}{(2\pi)^D} \int \frac{d^D k_E}{(k_E^2 + Q)^2} \quad (47)$$

where

$$Q = x^2 q^2 - x(q^2 + m_1^2 - m_2^2) + m_1^2 - i\varepsilon \quad (48)$$

is a constant with respect to the k_E -integration.

Also the 1-point integral A in (42) can be transformed into a Euclidean integral:

$$\frac{i}{16\pi^2} A(m) = -i \frac{\mu^{4-D}}{(2\pi)^D} \int \frac{d^D k_E}{k_E^2 + m^2}. \quad (49)$$

Both k_E - integrals are of the general type

$$\int \frac{d^D k_E}{(k_E^2 + L)^n}$$

of rotational-invariant integrals in a D -dimensional Euclidean space. They can be evaluated in D -dimensional polar coordinates ($k_E^2 = R$)

$$\int \frac{d^D k_E}{(k_E^2 + L)^n} = \frac{1}{2} \int d\Omega_D \int_0^\infty dR R^{\frac{D}{2}-1} \frac{1}{(R+L)^n},$$

yielding

$$\frac{\mu^{4-D}}{(2\pi)^D} \int \frac{d^D k_E}{(k_E^2 + L)^n} = \frac{\mu^{4-D}}{(4\pi)^{D/2}} \cdot \frac{\Gamma(n - \frac{D}{2})}{\Gamma(n)} \cdot L^{-n + \frac{D}{2}}. \quad (50)$$

The singularities of our initially 4-dimensional integrals are now recovered as poles of the Γ -function for $D = 4$ and values $n \leq 2$.

¹ The $i\varepsilon$ -prescription in the masses ensures that this is compatible with the pole structure of the integrand.

Although the l.h.s. of Eq. (50) as a D -dimensional integral is sensible only for integer values of D , the r.h.s. has an analytic continuation in the variable D : it is well defined for all complex values D with $n - \frac{D}{2} \neq 0, -1, -2, \dots$, in particular for

$$D = 4 - \epsilon \quad \text{with } \epsilon > 0.$$

For physical reasons we are interested in the vicinity of $D = 4$. Hence we consider the limiting case $\epsilon \rightarrow 0$ and perform an expansion around $D = 4$ in powers of ϵ . For this task we need the following properties of the Γ -function at $x \rightarrow 0$:

$$\begin{aligned} \Gamma(x) &= \frac{1}{x} - \gamma + O(x), \\ \Gamma(-1 + x) &= -\frac{1}{x} + \gamma - 1 + O(x) \end{aligned} \quad (51)$$

with

$$\gamma = -\Gamma'(1) = 0.577\dots$$

known as Euler's constant.

$n = 1$:

Combining (49) and (50) we obtain the scalar 1-point integral for $D = 4 - \epsilon$:

$$\begin{aligned} A(m) &= -\frac{\mu^\epsilon}{(4\pi)^{-\epsilon/2}} \cdot \frac{\Gamma(-1 + \frac{\epsilon}{2})}{\Gamma(1)} \cdot \left(m^2\right)^{1-\epsilon/2} \\ &= m^2 \left(\frac{2}{\epsilon} - \gamma + \log 4\pi - \log \frac{m^2}{\mu^2} + 1 \right) + O(\epsilon) \\ &\equiv m^2 \left(\Delta - \log \frac{m^2}{\mu^2} + 1 \right) + O(\epsilon) \end{aligned} \quad (52)$$

Here we have introduced the abbreviation for the singular part

$$\Delta = \frac{2}{\epsilon} - \gamma + \log 4\pi. \quad (53)$$

$n = 2$:

For the scalar 2-point integral B_0 we evaluate the integrand of the x -integration in Eq. (46) with help of Eq. (50) as follows:

$$\begin{aligned} \frac{\mu^\epsilon}{(4\pi)^{2-\epsilon/2}} \cdot \frac{\Gamma(\frac{\epsilon}{2})}{\Gamma(2)} \cdot Q^{-\epsilon/2} &= \frac{1}{16\pi^2} \left(\frac{2}{\epsilon} - \gamma + \log 4\pi - \log \frac{Q}{\mu^2} \right) + O(\epsilon) \\ &= \frac{1}{16\pi^2} \left(\Delta - \log \frac{Q}{\mu^2} \right) + O(\epsilon). \end{aligned} \quad (54)$$

Since the $O(\epsilon)$ terms vanish in the limit $\epsilon \rightarrow 0$ we skip them in the following formulae. Insertion into Eq. (46) with Q from Eq. (48) yields:

$$B_0(q^2, m_1, m_2) = \Delta - \int_0^1 dx \log \frac{x^2 q^2 - x(q^2 + m_1^2 - m_2^2) + m_1^2 - i\epsilon}{\mu^2}. \quad (55)$$

The explicit analytic formula can be found e.g. in [10].

For the calculation of one-loop amplitudes also 3- and 4-point functions have to be included. In low energy processes, like muon decay or neutrino scattering, where the external momenta can be neglected in view of the internal gauge boson masses, the 3-point and 4-point integrals can immediately be reduced to 2-point integrals. The analytic results for the $\gamma(Z)ff$ vertices can be found in the literature [20]. Massive box diagrams are negligible around the Z resonance.

3.3. Vector boson self-energies

The diagrams contributing to the self energies of the photon, W , Z and the photon– Z transition contain fermion, vector boson, Higgs and ghost loops. Here we consider the fermion loops in more detail, since they yield the biggest contributions.

Photon self-energy. We give the expression for a single fermion with charge Q_f and mass m . The total contribution is obtained by summing over all fermions. Evaluating the fermion loop diagram we obtain

$$\begin{aligned}\Sigma^\gamma(q^2) &= \frac{\alpha}{\pi} Q_f^2 \left\{ -A(m) + \frac{q^2}{2} B_0(q^2, m, m) + 2 B_{22}(q^2, m, m) \right\} \\ &= \frac{\alpha}{3\pi} Q_f^2 \left\{ q^2 \left(\Delta - \log \frac{m^2}{\mu^2} \right) + (q^2 + 2m^2) \bar{B}_0(q^2, m, m) - \frac{q^2}{3} \right\}.\end{aligned}\quad (56)$$

\bar{B}_0 denotes the finite function in the following decomposition of (55) for equal masses,

$$B_0(q^2, m, m) = \Delta - \log \frac{m^2}{\mu^2} + \bar{B}_0(q^2, m, m). \quad (57)$$

The dimensionless quantity

$$\Pi^\gamma(q^2) = \frac{\Sigma^\gamma(q^2)}{q^2} \quad (58)$$

is usually denoted as the photon vacuum polarization. Simple expressions arise from Eq. (56) for special situations of practical interest:

- light fermions ($|q^2| \gg m^2$):

$$\Pi^\gamma(q^2) = \frac{\alpha}{3\pi} Q_f^2 \left(\Delta - \log \frac{m^2}{\mu^2} + \frac{5}{3} - \log \frac{|q^2|}{m^2} + i\pi \theta(q^2) \right) \quad (59)$$

- heavy fermions ($|q^2| \ll m^2$):

$$\Pi^\gamma(q^2) = \frac{\alpha}{3\pi} Q_f^2 \left(\Delta - \log \frac{m^2}{\mu^2} + \frac{q^2}{5m^2} \right) \quad (60)$$

Photon– Z mixing. Each charged fermion yields a contribution

$$\begin{aligned}\Sigma^Z(q^2) &= \\ &- \frac{\alpha}{3\pi} \frac{v_f Q_f}{2 s_W c_W} \left\{ q^2 \left(\Delta - \log \frac{m^2}{\mu^2} \right) + (q^2 + 2m^2) \bar{B}_0(q^2, m, m) - \frac{q^2}{3} \right\}.\end{aligned}\quad (61)$$

As in the photon case, the fermion-loop contribution vanishes for $q^2 = 0$.

Z and W self energies. We give the formulae for a single doublet, leptons or quarks, with m_\pm , Q_\pm , v_\pm , a_\pm denoting mass, charge, vector and axial vector coupling of the up(+) and the down(–) member. At the end, we have to perform the sum over the various doublets, including colour summation.

$$\Sigma^Z(q^2) = \frac{\alpha}{\pi} \sum_{f=+,-} \left\{ \frac{v_f^2 + a_f^2}{4 s_W^2 c_W^2} \left[2 B_{22}(q^2, m_f, m_f) + \frac{q^2}{2} B_0(q^2, m_f, m_f) \right] \right\}$$

$$\begin{aligned}
& -A(m_f)] - \frac{m_f^2}{8s_W^2 c_W^2} B_0(q^2, m_f^2, m_f^2) \} , \\
\Sigma^W(q^2) &= \frac{\alpha}{\pi} \cdot \frac{1}{4s_W^2} \{ 2B_{22}(q^2, m_+, m_-) - \frac{A(m_+) + A(m_-)}{2} \\
& \quad + \frac{q^2 - m_+^2 - m_-^2}{2} B_0(q^2, m_+, m_-) \} . \tag{62}
\end{aligned}$$

The one-loop contribution to the ρ parameter [11]

$$\Delta\rho = \frac{\Sigma^Z(0)}{M_Z^2} - \frac{\Sigma^W(0)}{M_W^2} \tag{63}$$

is finite as far as the leading fermion contribution is considered. For the top quark the expressions above yield

$$\Delta\rho = N_C \frac{\alpha}{16\pi s_W^2 c_W^2} \frac{m_t^2}{M_Z^2} . \tag{64}$$

3.4. Renormalization at one-loop order

The Lagrangian of the minimal $SU(2) \times U(1)$ model involves a certain number of free parameters which are not fixed by the theory. The definition of these parameters and their relation to measurable quantities is the content of a renormalization scheme. The parameters (or appropriate combinations) can be determined from specific experiments with help of the theoretical results for cross sections and lifetimes. After this procedure of defining the physical input, other observables can be predicted allowing verification or falsification of the theory by comparison with the corresponding experimental results.

In higher order perturbation theory the relations between the formal parameters and measurable quantities are different from the tree level relations in general. Moreover, the procedure is obscured by the appearance of divergences from the loop integrations. For a mathematically consistent treatment one has to regularize the theory, e.g. by dimensional regularization (performing the calculations in D dimensions). But then the relations between physical quantities and the parameters become cutoff dependent. Hence, the parameters of the basic Lagrangian, the “bare” parameters, have no physical meaning. The standard treatment is to replace the bare parameters by renormalized ones by writing for each parameter g_0

$$g_0 = Z_g g = g + \delta g \tag{65}$$

with a renormalization constants Z_g different from 1 by a one-loop term. The renormalized parameters g are finite and fixed by a set of renormalization conditions. The decomposition (65) is to a large extent arbitrary. Only the divergent parts are determined directly by the structure of the divergences of the one-loop amplitudes. The finite parts depend on the choice of the explicit renormalization conditions.

In QED and in the electroweak theory, classical Thomson scattering and the particle masses set natural scales where the parameters can be defined. In QED the favoured renormalization scheme is the on-shell scheme where $e = \sqrt{4\pi\alpha}$ and the electron mass are used as input parameters. In the electroweak Standard Model a distinguished set for parameter renormalization is given in terms of e, M_Z, M_W, M_H, m_f with the masses of the corresponding particles. This electroweak on-shell scheme is the straight-forward extension of the familiar QED renormalization, first proposed by Ross and Taylor [12] and used in many practical applications [6,10,13-21]. The mass of the Higgs boson, as long as it is experimentally unknown, is treated as a free input parameter. The light quark masses can only be considered as effective parameters.

In the cases of practical interest they can be replaced in terms of directly measured quantities like the cross section for $e^+e^- \rightarrow \text{hadrons}$.

Instead of choosing e , M_W , M_Z as basic free parameters one may alternatively use as basic parameters α , G_μ , M_Z [22] or α , G_μ , $\sin^2 \theta_W$ with the mixing angle deduced from neutrino-electron scattering [23] or perform the loop calculations in the \overline{MS} scheme [24-27]. The following discussion is based on the on-shell scheme.

Mass renormalization. The vector-boson masses are part of the propagators; we thus have to investigate the effects of the W and Z self-energies. We restrict our discussion to the transverse parts $\sim g_{\mu\nu}$. In the electroweak theory, differently from QED, the longitudinal components $\sim q_\mu q_\nu$ of the vector boson propagators do not give zero results in physical matrix elements. But for light external fermions the contributions are suppressed by $(m_f/M_Z)^2$ and we are allowed to neglect them. Writing the self-energies as

$$\Sigma_{\mu\nu}^{W,Z} = g_{\mu\nu} \Sigma^{W,Z} + \dots \quad (66)$$

with scalar functions $\Sigma^{W,Z}(q^2)$ we have for the one-loop propagators

$$\frac{-ig^{\mu\sigma}}{q^2 - M_V^2} \left(-i \Sigma_{\rho\sigma}^V \right) \frac{-ig^{\rho\nu}}{q^2 - M_V^2} = \frac{-ig^{\mu\nu}}{q^2 - M_V^2} \left(\frac{-\Sigma^V(q^2)}{q^2 - M_V^2} \right), \quad V = W, Z \quad (67)$$

(the factor $-i$ in the self energy insertion is a convention). Besides the fermion loop contributions in the electroweak theory there are also the non-Abelian gauge boson loops and loops involving the Higgs boson. The Higgs boson and the top quark thus enter the 4-fermion amplitudes as experimentally unknown objects at the level of radiative corrections and have to be treated as additional free parameters. In the graphical representation, the self-energies for the vector bosons denote the sum of all the diagrams with virtual fermions, vector bosons, Higgs and ghost loops. Resumming all self energy-insertions yields a geometrical series for the dressed propagators:

$$\begin{aligned} & \frac{-ig_{\mu\nu}}{q^2 - M_V^2} \left[1 + \left(\frac{-\Sigma^V}{q^2 - M_V^2} \right) + \left(\frac{-\Sigma^V}{q^2 - M_V^2} \right)^2 + \dots \right] \\ &= \frac{-ig_{\mu\nu}}{q^2 - M_V^2 + \Sigma^V(q^2)}. \end{aligned} \quad (68)$$

The self-energies have the following properties:

- $\text{Im}\Sigma^V(M_V^2) \neq 0$ for both W and Z . This is because W and Z are unstable particles and can decay into pairs of light fermions. The imaginary parts correspond to the total decay widths of W , Z and remove the poles from the real axis.
- $\text{Re}\Sigma^V(M_V^2) \neq 0$ for both W and Z and they are UV divergent.

The second feature tells us that the locations of the poles in the propagators are shifted by the loop contributions. Consequently, the principal step in mass renormalization consists in a re-interpretation of the parameters: the masses in the Lagrangian cannot be the physical masses of W and Z but are the bare masses, related to the physical masses M_W , M_Z by

$$\begin{aligned} M_W^{0,2} &= M_W^2 + \delta M_W^2 \\ M_Z^{0,2} &= M_Z^2 + \delta M_Z^2 \end{aligned} \quad (69)$$

with counterterms of one-loop order. The correct propagators according to this prescription are given by

$$\frac{-ig_{\mu\nu}}{q^2 - M_V^{0,2} + \Sigma^V(q^2)} = \frac{-ig_{\mu\nu}}{q^2 - M_V^2 - \delta M_V^2 + \Sigma^V(q^2)} \quad (70)$$

instead of Eq. (45). The renormalization conditions which ensure that $M_{W,Z}$ are the physical masses fix the mass counterterms to be

$$\begin{aligned}\delta M_W^2 &= \text{Re } \Sigma^W(M_W^2) \\ \delta M_Z^2 &= \text{Re } \Sigma^Z(M_Z^2).\end{aligned}\quad (71)$$

In this way, two of our input parameters and their counterterms have been defined. From the photon self-energy $\Sigma^\gamma(q^2)$ no mass term arises for the photon since it behaves like

$$\Sigma^\gamma(q^2) \simeq q^2 \Pi^\gamma(0)$$

for $q^2 \rightarrow 0$ leaving the pole at $q^2 = 0$ in the propagator. The absence of mass terms for the photon in all orders is a consequence of the unbroken electromagnetic gauge invariance.

Charge renormalization. Our third input parameter is the electromagnetic charge e . The electroweak charge renormalization is very similar to that in pure QED. As in QED, we want to maintain the definition of e as the classical charge in the Thomson cross section. Accordingly, the Lagrangian carries the bare charge $e_0 = e + \delta e$ with the charge counter term δe of one-loop order. The charge counter term δe has to absorb the electroweak loop contributions to the $ee\gamma$ vertex in the Thomson limit. This charge-renormalization condition is simplified by the validity of a generalization of the QED Ward identity [28] which implies that those corrections related to the external particles cancel each other. Thus for δe only two universal contributions are left:

$$\frac{\delta e}{e} = \frac{1}{2} \Pi^\gamma(0) - \frac{s_W}{c_W} \frac{\Sigma^{\gamma Z}(0)}{M_Z^2}.\quad (72)$$

The first term, quite in analogy to QED, is given by the vacuum polarization of the photon. But now, besides the fermion loops, it contains also bosonic loop diagrams from W^+W^- virtual states and the corresponding ghosts. The second term contains the mixing between photon and Z , in general described as a mixing propagator, with $\Sigma^{\gamma Z}$ normalized as

$$\Delta_{\mu\nu}^{\gamma Z} = \frac{-ig_{\mu\nu}}{q^2} \left(\frac{-\Sigma^{\gamma Z}(q^2)}{q^2 - M_Z^2} \right).$$

The fermion loop contributions to $\Sigma^{\gamma Z}$ vanish at $q^2 = 0$; only the non-Abelian bosonic loops yield $\Sigma^{\gamma Z}(0) \neq 0$.

In summary, for electroweak one-loop calculations \mathcal{L} has to be considered as the bare Lagrangian of the theory $\mathcal{L}(e_0, M_W^0, M_Z^0, \dots)$ with bare parameters, which are related to the physical ones by

$$e_0 = e + \delta e, \quad M_W^{02} = M_W^2 + \delta M_W^2, \quad M_Z^{02} = M_Z^2 + \delta M_Z^2.\quad (73)$$

The counter terms are fixed in terms of a certain subset of 1-loop diagrams by specifying the definition of the physical parameters. For any 4-fermion process we can write down the 1-loop matrix element with the bare parameters and the loop diagrams for this process. Together with the counter terms the matrix element is finite when expressed in terms of the physical parameters, i.e. all UV singularities are removed.

4. The vector boson masses at higher order

4.1. One-loop corrections to the muon lifetime

The interdependence between the gauge boson masses M_W, M_Z is established through the accurately measured muon lifetime or, equivalently, the Fermi constant G_μ , in lowest order

given by Eq. (24). Originally, the μ lifetime τ_μ was calculated within the framework of the effective four-point Fermi interaction. Beyond the long-standing one-loop QED corrections [29], the two-loop QED corrections in the Fermi model have also become available [30], yielding the expression (the error in the two-loop term is from the hadronic uncertainty)

$$\frac{1}{\tau_\mu} = \frac{G_\mu^2 m_\mu^5}{192\pi^3} \left(1 - \frac{8m_e^2}{m_\mu^2}\right) \cdot K_{\text{QED}},$$

$$K_{\text{QED}} = 1 + 1.810 \frac{\alpha(m_\mu)}{\pi} + (6.701 \pm 0.002) \left(\frac{\alpha(m_\mu)}{\pi}\right)^2. \quad (74)$$

This formula is the defining equation for G_μ in terms of the experimental μ lifetime, from which the value in Eq. (23) is obtained [30].

In higher order, G_μ is given by the expression

$$\frac{G_\mu}{\sqrt{2}} = \frac{e_0^2 \sqrt{2}}{8s_W^{0.2} M_W^{0.2}} \left[1 + \frac{\Sigma^W(0)}{M_W^2} + (\text{vertex, box}) \right] \quad (75)$$

involving the the bare parameters (73) and the bare mixing angle $s_W^{0.2}$ in (76); the vertex corrections and box diagrams in the decay amplitude are indicated by the term *(vertex, box)*. Thereby, a set of infra-red divergent QED-correction graphs has to be removed. These omitted diagrams, together with the real bremsstrahlung contributions, reproduce the QED-correction factor of the Fermi-model result in Eq. (74); they have no influence on the relation between G_μ and the Standard Model parameters and are not part of (75).

Evaluating Eq. (75) to one-loop order by expanding the bare parameters (73) to first order in the counterterms, including

$$s_W^{0.2} = 1 - \frac{M_W^{0.2}}{M_Z^{0.2}} = s_W^2 + c_W^2 \left(\frac{\delta M_Z^2}{M_Z^2} - \frac{\delta M_W^2}{M_W^2} \right), \quad (76)$$

and keeping only terms of one-loop order in Eq. (75) yields

$$\frac{G_\mu}{\sqrt{2}} = \frac{e^2}{8s_W^2 M_W^2} \cdot$$

$$\cdot \left[1 + 2 \frac{\delta e}{e} - \frac{c_W^2}{s_W^2} \left(\frac{\delta M_Z^2}{M_Z^2} - \frac{\delta M_W^2}{M_W^2} \right) + \frac{\Sigma^W(0) - \delta M_W^2}{M_W^2} + (\text{vertex, box}) \right]$$

$$\equiv \frac{e^2}{8s_W^2 M_W^2} \cdot [1 + \Delta r], \quad (77)$$

the one-loop version of Eq. (24), first calculated in [14]. The quantity Δr is a finite combination of loop diagrams and counterterms. Inserting the counterterms from the previous section and adding the vertex and box contributions one obtains

$$\Delta r = \Pi^\gamma(0) - \frac{c_W^2}{s_W^2} \left(\frac{\delta M_Z^2}{M_Z^2} - \frac{\delta M_W^2}{M_W^2} \right) + \frac{\Sigma^W(0) - \delta M_W^2}{M_W^2}$$

$$+ 2 \frac{c_W}{s_W} \frac{\Sigma^{\gamma Z}(0)}{M_Z^2} + \frac{\alpha}{4\pi s_W^2} \left(6 + \frac{7 - 4s_W^2}{2s_W^2} \log c_W^2 \right). \quad (78)$$

$\Delta r = \Delta r(e, M_W, M_Z, M_H, m_t)$ depends on the entire set of on-shell parameters. The mass of the Higgs boson M_H enters, as an experimentally unknown parameter, via the vector boson self-energies.

4.2. Light and heavy fermions

The photon vacuum polarization is a basic entry in the predictions for electroweak precision observables. The difference

$$\text{Re } \hat{\Pi}^\gamma(M_Z^2)) = \text{Re } \Pi^\gamma(M_Z^2) - \Pi^\gamma(0) \quad (79)$$

is a finite quantity. The purely fermionic part corresponds to standard QED and does not depend on the details of the electroweak theory. It can be split into a leptonic and a hadronic contribution

$$\text{Re } \hat{\Pi}^\gamma(M_Z^2)_{\text{ferm}} = \text{Re } \hat{\Pi}_{\text{lept}}^\gamma(M_Z^2) + \text{Re } \hat{\Pi}_{\text{had}}^\gamma(M_Z^2). \quad (80)$$

The top quark is by convention not included in the hadronic part; according to Eq. (60) it provides a small non-logarithmic additional contribution

$$\hat{\Pi}_{\text{top}}^\gamma(M_Z^2) \simeq \frac{\alpha}{\pi} Q_t^2 \frac{M_Z^2}{5 m_t^2} \simeq 0.6 \cdot 10^{-4}. \quad (81)$$

The quantity

$$\begin{aligned} \Delta\alpha &= \Delta\alpha_{\text{lept}} + \Delta\alpha_{\text{had}} \\ &= -\text{Re } \hat{\Pi}_{\text{lept}}^\gamma(M_Z^2) - \text{Re } \hat{\Pi}_{\text{had}}^\gamma(M_Z^2) \end{aligned} \quad (82)$$

represents a QED-induced shift in the electromagnetic fine structure constant

$$\alpha \rightarrow \alpha(1 + \Delta\alpha), \quad (83)$$

which can be resummed according to the renormalization group, accommodating all the leading logarithms of the type $\alpha^n \log^n(M_Z/m_f)$. The result is an effective fine structure constant at the Z mass scale:

$$\alpha(M_Z^2) = \frac{\alpha}{1 - \Delta\alpha}. \quad (84)$$

It corresponds to a resummation of the iterated 1-loop vacuum polarization from the light fermions to all orders.

$\Delta\alpha$ is an input of crucial importance because of its universality and of its remarkable size of ~ 0.06 . The leptonic content can be directly evaluated in terms of the known lepton masses, yielding at one loop order from Eq. (59)

$$\Delta\alpha_{\text{lept}} = \sum_{\ell=e,\mu,\tau} \frac{\alpha}{3\pi} \left(\log \frac{M_Z^2}{m_\ell^2} - \frac{5}{3} \right) + \mathcal{O}\left(\frac{m_\ell^2}{M_Z^2}\right). \quad (85)$$

The 2-loop correction has been known already for a long time [31], and also the 3-loop contribution is now available [32], yielding altogether

$$\Delta\alpha_{\text{lept}} = 314.97687 \cdot 10^{-4}. \quad (86)$$

For the light hadronic part, perturbative QCD is not applicable and quark masses are no reasonable input parameters. Instead, the 5-flavour contribution to $\hat{\Pi}_{\text{had}}^\gamma$ can be derived from experimental data with the help of a dispersion relation

$$\Delta\alpha_{\text{had}} = -\frac{\alpha}{3\pi} M_Z^2 \text{Re} \int_{4m_\pi^2}^{\infty} ds' \frac{R^\gamma(s')}{s'(s' - M_Z^2 - i\varepsilon)} \quad (87)$$

with

$$R^\gamma(s) = \frac{\sigma(e^+e^- \rightarrow \gamma^* \rightarrow \text{hadrons})}{\sigma(e^+e^- \rightarrow \gamma^* \rightarrow \mu^+\mu^-)}$$

as an experimental input quantity for low energy range. Integrating over data for the low-energy range and applying perturbative QCD for the high-energy region above, the expression (87) yields the value [33,34]

$$\Delta\alpha_{\text{had}} = -0.02758 \pm 0.00035. \quad (88)$$

Because of the lack of precision in the experimental data a large uncertainty is associated with the value of $\Delta\alpha_{\text{had}}$, which propagates into the theoretical error of the predictions of electroweak precision observables.

The contribution from the heavy quark doublet (t, b) to Δr , utilizing the formulae of section 3.3, can be written in the following way as far as the leading terms are concerned:

$$(\Delta r)_{b,t} = -\text{Re}\hat{\Pi}_b^\gamma(M_Z^2) - \frac{c_W^2}{s_W^2} \Delta\rho + \dots \quad (89)$$

with $\Delta\rho$ from Eq. (64). The first term is the b -quark contribution to the effective charge and is already contained in $\Delta\alpha$.

Thus we have got a simple form for Δr with respect to the the light- and heavy-fermion terms:

$$\Delta r = \Delta\alpha - \frac{c_W^2}{s_W^2} \Delta\rho + (\Delta r)_{\text{remainder}}. \quad (90)$$

$\Delta\alpha$ contains the large logarithmic corrections from the light fermions and $\Delta\rho$ the leading quadratic correction from a large top mass. All other terms are collected in the $(\Delta r)_{\text{remainder}}$. It should be noted that the remainder also contains a term logarithmic in the top mass (for which our approximation above was too crude) which is not negligible

$$(\Delta r)_{\text{remainder}}^{\text{top}} = -\frac{\alpha}{4\pi s_W^2} \left(\frac{c_W^2}{s_W^2} - \frac{1}{3} \right) \log \frac{m_t}{M_Z} + \dots \quad (91)$$

Also the Higgs boson contribution is part of the remainder. For large M_H , it increases only logarithmically (“screening” of a heavy Higgs [35]):

$$(\Delta r)_{\text{remainder}}^{\text{Higgs}} \simeq \frac{\alpha}{16\pi s_W^2} \cdot \frac{11}{3} \left(\log \frac{M_H^2}{M_W^2} - \frac{5}{6} \right). \quad (92)$$

The typical size of $(\Delta r)_{\text{remainder}}$ is of the order ~ 0.01 .

4.3. Higher order contributions

(i) Summation of large $\Delta\alpha$ terms: The replacement of the $\Delta\alpha$ -part

$$1 + \Delta\alpha \rightarrow \frac{1}{1 - \Delta\alpha}$$

of the 1-loop result in Eq. (87) correctly takes into account all orders in the leading logarithmic corrections $(\Delta\alpha)^n$, as can be shown by renormalization group arguments [36]. The evolution of the electromagnetic coupling with the scale μ is described by the renormalization group equation

$$\mu \frac{d\alpha}{d\mu} = -\frac{\beta_0}{2\pi} \alpha^2 \quad (93)$$

with the coefficient of the 1-loop β -function in QED

$$\beta_0 = -\frac{4}{3} \sum_{f \neq t} Q_f^2. \quad (94)$$

The solution of the RGE contains the leading logarithms in the resummed form. It corresponds to the replacement $\alpha \rightarrow \alpha(M_Z^2)$, see eq. (84). It corresponds to a resummation of the iterated 1-loop vacuum polarization to all orders.

(ii) Summation of large $\Delta\rho$ terms: Since the top quark is heavy, also $\Delta\rho$ is large and powers of $(\Delta\rho)$ are not negligible. A result correct in the leading terms up to $O(\alpha^2)$ is given by the independent resummation [37]

$$\frac{1}{1 - \Delta r} \rightarrow \frac{1}{1 - \Delta\alpha} \cdot \frac{1}{1 + \frac{c_W^2}{s_W^2} \Delta\bar{\rho}} + (\Delta r)_{\text{remainder}} \quad (95)$$

where

$$\Delta\bar{\rho} = 3x_t[1 + \delta\rho^{(2)} + \delta\rho^{(3)}], \quad x_t = \frac{G_\mu m_t^2}{8\pi^2 \sqrt{2}} \quad (96)$$

incorporates the result from electroweak two-loop [38-40] and three-loop [41,42] one-particle-irreducible diagrams. With the resummed ρ -parameter

$$\rho = \frac{1}{1 - \Delta\bar{\rho}}, \quad (97)$$

Eq. (95) is compatible with the following form of the M_W – M_Z interdependence

$$G_\mu = \frac{\pi}{\sqrt{2}} \frac{\alpha(M_Z^2)}{M_W^2 \left(1 - \frac{M_W^2}{\rho M_Z^2}\right)} \cdot [1 + (\Delta r)_{\text{remainder}}], \quad (98)$$

with $\alpha(M_Z^2)$ in (84). It is interesting to compare this result with the corresponding lowest order M_W – M_Z correlation in a more general model with a tree level ρ -parameter $\rho_0 \neq 1$: the tree-level ρ_0 enters in the same way as the ρ from a heavy top in the minimal model. In the minimal model, however, ρ is calculable in terms of m_t , M_H whereas ρ_0 is an *additional* free parameter.

(iii) QCD corrections: Virtual gluons contribute to the quark loops in the vector boson self-energies from the 2-loop level on. For the light quarks this QCD correction is already contained in the result for the hadronic vacuum polarization from the dispersion integral, Eq. (93). Fermion loops involving the top quark get additional $O(\alpha\alpha_s)$ corrections which have been calculated perturbatively [46]. The dominating term represents the QCD correction to the leading m_t^2 term of the ρ -parameter and can be incorporated by writing instead of Eq. (96):

$$\Delta\bar{\rho} = 3x_t \cdot [1 + \rho^{(2)} + \rho^{(3)} + \delta\rho_{\text{QCD}}] \quad (99)$$

The QCD term contributions [41,43-45] reads:

$$\delta\rho_{\text{QCD}} = -\frac{\alpha_s(\mu)}{\pi} c_1 + \left(\frac{\alpha_s(\mu)}{\pi}\right)^2 c_2(\mu) + \dots \quad (100)$$

with

$$c_1 = \frac{2}{3} \left(\frac{\pi^2}{3} + 1\right) = 2.8599 \quad (101)$$

and the three-loop coefficient [44]

$$c_2 = -14.59 \text{ for } \mu = m_t \text{ and 6 flavors} \quad (102)$$

with the on-shell top mass m_t . The dots indicate higher-order QCD and mixed electroweak-QCD terms [41,45]. As part of the higher order irreducible contributions to ρ , the QCD correction is resummed together with the electroweak 2-loop irreducible term as indicated in Eq. (95).

Beyond the $G_\mu m_t^2 \alpha_s$ approximation through the ρ -parameter, the complete $O(\alpha \alpha_s)$ corrections to the self energies are available from perturbative calculations [46] and by means of dispersion relations [47]. Also non-leading terms to Δr of $O(\alpha_s^2)$ have been computed [48].

- (iv) Non-leading electroweak two-loop terms: During the last years, the complete electroweak two-loop result in the Standard Model for Δr has become available: the fermionic two-loop terms [49] with all two-loop diagrams for the muon-decay amplitude containing at least one closed fermion loop, and the residual class of the two-loop purely bosonic diagrams [50,51]. Their influence is displayed in Figure 1 for the fermionic and in Figure 2 for the bosonic contributions, in terms of Δr and M_W .

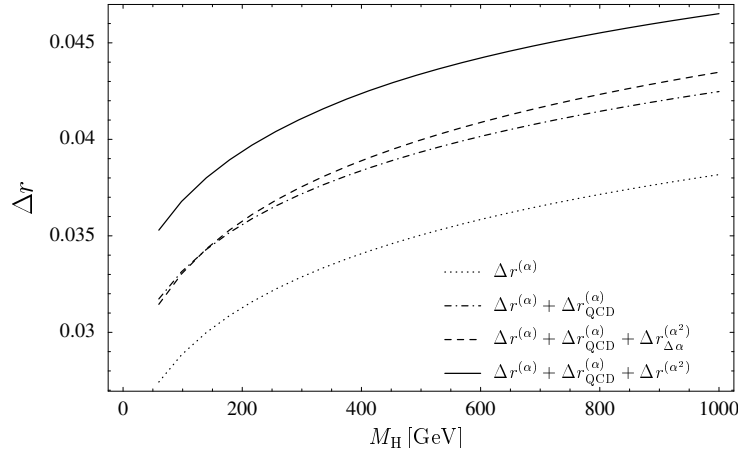


Figure 1. Various stages of Δr , as a function of M_H . The one-loop contribution, $\Delta r^{(\alpha)}$, is supplemented by the two-loop and three-loop QCD corrections, $\Delta r_{\text{QCD}}^{(\alpha)} \equiv \Delta r^{(\alpha \alpha_s)} + \Delta r^{(\alpha \alpha_s^2)}$, and the fermionic electroweak two-loop contributions, $\Delta r^{(\alpha^2)} \equiv \Delta r^{(N_f \alpha^2)} + \Delta r^{(N_f^2 \alpha^2)}$. For comparison, the effect of the two-loop corrections induced by a resummation of $\Delta \alpha$, $\Delta r_{\Delta \alpha}^{(\alpha^2)}$, is shown separately.

5. Z boson observables

5.1. Effective Z couplings

A gauge invariant subset of the 1-loop diagrams to $e^+ e^- \rightarrow f \bar{f}$ are the QED corrections: The sum of the virtual photon loop graphs is UV finite but IR (= infra-red) divergent because of the massless photon. The IR-divergence is cancelled by adding the cross section with real photon bremsstrahlung (after integrating over the phase space for experimentally invisible photons) which always accompanies a realistic scattering process. Since the phase space for invisible photons is a detector dependent quantity the QED corrections cannot in general be separated from the experimental device.

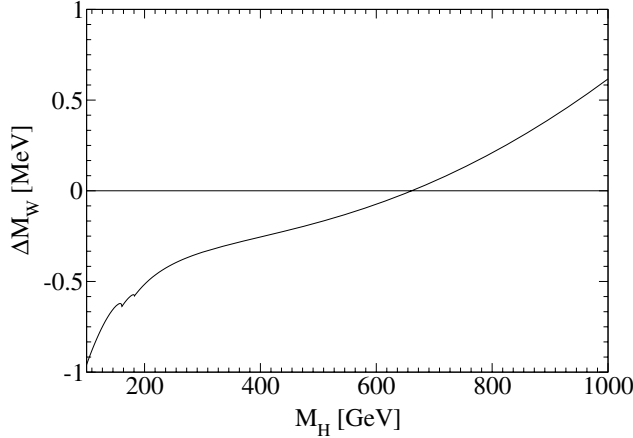


Figure 2. The shift in M_W from the two-loop bosonic contributions to Δr (from [50]).

The residual diagrams form the non-QED or weak corrections. This class is free of IR-singularities but sensitive to the details beyond the lowest order amplitudes. The UV-singular terms associated with the loop diagrams are cancelled by our counterterms of section 3.4, as a consequence of renormalizability. The 1-loop amplitude for $e^+e^- \rightarrow f\bar{f}$ contains the sum of the individual contributions to the self-energies and vertex corrections (including the external fermion self-energies via wave function renormalization). The essential steps for getting the total amplitude finite are: expressing the tree diagrams in terms of the bare parameters e_0 , $M_Z^{0,2}$, $s_W^{0,2}$ expanding the bare quantities according to Eqs. (73,76) and adding the loop diagrams. The total amplitude around the Z pole can be written as the sum of a dressed photon and a dressed Z -exchange amplitude; box diagrams are numerically not significant around the peak (relative contribution $< 10^{-4}$). For a review see [52].

The Z -exchange amplitude with effective vertices can be written in the following way:

$$A_Z = \frac{\langle J_\mu^{(e)} \rangle \otimes \langle J^{(f)\mu} \rangle}{s - M_Z^2 + i s \Gamma_Z / M_Z}. \quad (103)$$

The s -dependence of the imaginary part is due to the s -dependence of $\text{Im } \Sigma^Z$; the linearization is completely sufficient in the resonance region.

The factorized Z amplitude (103) contains the fermionic matrixelements of the neutral current vertices with effective coupling constants $g_{V,A}^f$, or synonymously with form factors ρ_f and κ_f :

$$\begin{aligned} J_\mu^{(f)} &= \left(\sqrt{2} G_\mu M_Z^2 \rho_f \right)^{1/2} \left[(I_3^f - 2 Q_f s_W^2 \kappa_f) \gamma_\mu - I_3^f \gamma_\mu \gamma_5 \right] \\ &= \left(\sqrt{2} G_\mu M_Z^2 \right)^{1/2} [g_V^f \gamma_\mu - g_A^f \gamma_\mu \gamma_5]. \end{aligned} \quad (104)$$

The expressions for the effective couplings are given by

$$\begin{aligned} g_V^f &= \left[v_f + 2 s_W c_W Q_f \frac{\hat{\Pi}^{\gamma Z}(M_Z^2)}{1 + \hat{\Pi}^\gamma(M_Z^2)} + F_V^{Zf} \right] \left(\frac{1 - \Delta r}{1 + \hat{\Pi}^Z(M_Z^2)} \right)^{1/2}, \\ g_A^f &= \left[a_f + F_A^{Zf} \right] \left(\frac{1 - \Delta r}{1 + \hat{\Pi}^Z(M_Z^2)} \right)^{1/2}. \end{aligned} \quad (105)$$

The entries are the following finite combinations of 2-point functions, evaluated at $s = M_Z^2$, together with Δr ,

$$\begin{aligned}\hat{\Pi}^Z(s) &= \frac{\text{Re } \Sigma^Z(s) - \delta M_Z^2}{s - M_Z^2} - \Pi^\gamma(0) + \\ &\quad \frac{c_W^2 - s_W^2}{s_W^2} \left(\frac{\delta M_Z^2}{M_Z^2} - \frac{\delta M_W^2}{M_W^2} - 2 \frac{s_W}{c_W} \frac{\Sigma^{\gamma Z}(0)}{M_Z^2} \right), \\ \hat{\Pi}^{\gamma Z}(s) &= \frac{\Sigma^{\gamma Z}(s) - \Sigma^{\gamma Z}(0)}{s} - \frac{c_W}{s_W} \left(\frac{\delta M_Z^2}{M_Z^2} - \frac{\delta M_W^2}{M_W^2} \right) + 2 \frac{\Sigma^{\gamma Z}(0)}{M_Z^2}\end{aligned}\quad (106)$$

and the finite vector and axial vector form factors $F_{V,A}$ at $s = M_Z^2$ in the vertex corrections including also the external fermion wave function renormalizations, which can be written as

$$i \frac{e}{2s_W c_W} \left[\gamma_\mu F_V^{Zf}(s) - \gamma_\mu \gamma_5 F_A^{Zf}(s) + I_3^f \gamma_\mu (1 - \gamma_5) \cdot \frac{c_W}{s_W} \frac{\Sigma^{\gamma Z}(0)}{M_Z^2} \right]. \quad (107)$$

Owing to the imaginary parts of the self-energies and vertices, the form factors and the effective couplings, respectively, are complex quantities. The approximation, where the couplings are taken as real, is called the “improved Born approximation”. For the full expressions see [20].

The leading structure of the universal parts can easily be understood from the counter term expansion in the tree-level amplitude with pure parameters:

$$\begin{aligned}\frac{e_0^2}{4s_W^0 c_W^0} &= \frac{e^2}{4s_W^2 c_W^2} \left[1 + 2 \frac{\delta e}{e} - \frac{c_W^2 - s_W^2}{s_W^2} \left(\frac{\delta M_Z^2}{M_Z^2} - \frac{\delta M_W^2}{M_W^2} \right) \right] \\ &= \sqrt{2} G_\mu M_Z^2 \left[1 + \frac{\delta M_Z^2}{M_Z^2} - \frac{\delta M_W^2}{M_W^2} + \dots \right]\end{aligned}$$

and

$$\frac{\delta M_Z^2}{M_Z^2} - \frac{\delta M_W^2}{M_W^2} = \Delta\rho + \dots$$

in the quadratic m_t -term. Thereby, G_μ was introduced by means of Eq. (87) together with the expression (98) for Δr , which cancels the $\Delta\alpha$ term. In a similar way one finds from Eq. (76):

$$s_W^{02} = s_W^2 \left[1 + \frac{c_W^2}{s_W^2} \left(\frac{\delta M_Z^2}{M_Z^2} - \frac{\delta M_W^2}{M_W^2} \right) \right] = s_W^2 \left[1 + \frac{c_W^2}{s_W^2} \Delta\rho + \dots \right],$$

where the term in brackets is part of the κ_f term in Eq. (106).

The Zbb couplings: The b -quark couplings contain a non-universal part with a strong dependence on m_t [53] resulting from the virtual top quark in the vertex corrections. The difference between the d and b couplings can be parametrized in the following way

$$\rho_b = \rho_d(1 + \tau)^2, \quad s_b^2 = s_d^2(1 + \tau)^{-1} \quad (108)$$

with the quantity

$$\tau = \Delta\tau^{(1)} + \Delta\tau^{(2)} + \Delta\tau^{(\alpha_s)}$$

calculated perturbatively, including the complete 1-loop order term [53], with x_t from Eq. (96)

$$\Delta\tau^{(1)} = -2x_t - \frac{G_\mu M_Z^2}{6\pi^2 \sqrt{2}} (c_W^2 + 1) \log \frac{m_t}{M_W} + \dots, \quad (109)$$

and the leading electroweak 2-loop contribution of $O(G_\mu^2 m_t^4)$ [39,54]

$$\Delta\tau^{(2)} = -2x_t^2 \tau^{(2)}, \quad (110)$$

where $\tau^{(2)}$ is a function of M_H/m_t with $\tau^{(2)} = 9 - \pi^2/3$ for small M_H .

5.2. Mixing angles and asymmetries

The effective mixing angles

$$s_f^2 = s_W^2 \operatorname{Re} \kappa_f$$

are of particular interest, since they determine the on-resonance asymmetries via the combinations of coupling constants (the imaginary parts are dropped)

$$A_f = \frac{2g_V^f g_A^f}{(g_V^f)^2 + (g_A^f)^2}, \quad (111)$$

which contain the ratios

$$g_V^f/g_A^f = 1 - 2Q_f s_f^2. \quad (112)$$

Of special interest are:

– the forward–backward asymmetry

$$A_{\text{FB}}^f = \frac{\sigma_F - \sigma_B}{\sigma_F + \sigma_B} \quad (113)$$

with (θ denotes the scattering angle)

$$\sigma_F = \int_{\theta > \pi/2} d\Omega \frac{d\sigma}{d\Omega}, \quad \sigma_B = \int_{\theta < \pi/2} d\Omega \frac{d\sigma}{d\Omega}. \quad (114)$$

Without QED corrections, photon-exchange and Z –photon interference terms, it is given by

$$A_{\text{FB}}^{0f} = \frac{3}{4} A_e A_f. \quad (115)$$

– the longitudinal polarization of a final-state τ lepton

$$P_\tau^{\text{pol}} = A_\tau, \quad (116)$$

– the left–right asymmetry

$$A_{\text{LR}} = \frac{\sigma_L - \sigma_R}{\sigma_L + \sigma_R} \cdot \frac{1}{\mathcal{P}_e} \quad (117)$$

with the cross section $\sigma_{L(R)}$ for longitudinally polarized, left(right)-handed, initial state electrons, with the degree of polarization \mathcal{P}_e . Without QED corrections, photon-exchange and Z –photon interference terms, the on-resonance asymmetry is given by

$$A_{\text{LR}}^0 = A_e. \quad (118)$$

The leptonic mixing angle, $s_e^2 \equiv \sin \theta_{\text{eff}}$, usually labeled as the genuine effective mixing angle, plays a special role as a particularly precise observable with a high sensitivity to the Higgs-boson mass. For this reason, a prediction of at least two-loop accuracy is necessary, beyond the already known terms through $\Delta\rho$ and QCD. Quite recently, complete electroweak two-loop calculations have been accomplished [55]. The effects of the higher-order contributions are visualized in Figure 3.

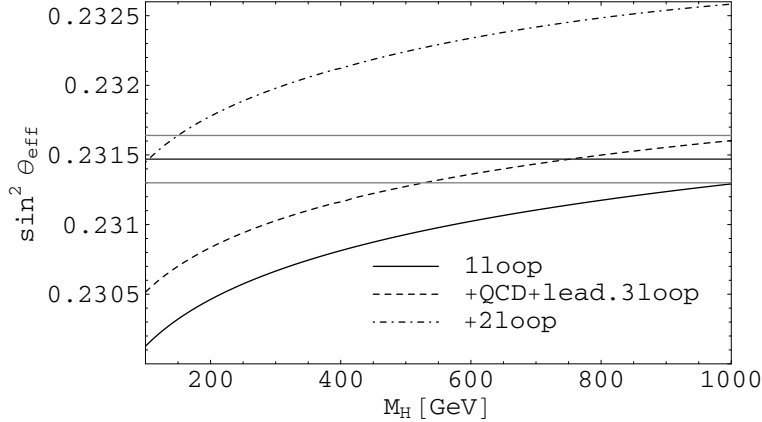


Figure 3. The leptonic effective mixing angle with higher-order contributions.

5.3. Z line-shape and Z widths

The integrated cross section $\sigma(s)$ for $e^+e^- \rightarrow f\bar{f}$ around the Z resonance with unpolarized beams is obtained from the formulae of the previous section in a straight forward way, expressed in terms of the effective vector and axial vector coupling constants. It is, however, convenient to rewrite $\sigma(s)$ in terms of the Z width and the partial widths Γ_e , Γ_f in order to have a more model independent expression.

We concentrate on the pure Z -resonance term. It differs from a Breit-Wigner line-shape by the s -dependence of the width. Denoting by Γ_Z the total width, the pure Z -resonance part of the integrated cross section for $e^+e^- \rightarrow f\bar{f}$ has the form

$$\sigma_{\text{res}}(s) = \sigma_0 \frac{s\Gamma_Z^2}{(s - M_Z^2)^2 + s^2\Gamma_Z^2/M_Z^2}, \quad \sigma_0 = \frac{12\pi}{M_Z^2} \cdot \frac{\Gamma_e\Gamma_f}{\Gamma_Z^2}. \quad (119)$$

The s -dependent width gives rise to a dislocation of the peak maximum by $\simeq -34$ GeV [56,57]. By means of the substitution [57]

$$s - M_Z^2 + is\Gamma_Z/M_Z = (1 + i\gamma)(s - \hat{M}_Z^2 + i\hat{M}_Z\hat{\Gamma}_Z) \quad (120)$$

with

$$\hat{M}_Z = M_Z(1 + \gamma^2)^{-1/2}, \quad \hat{\Gamma}_Z = \Gamma_Z(1 + \gamma^2)^{-1/2}, \quad \gamma = \frac{\Gamma_Z}{M_Z} \quad (121)$$

a genuine Breit-Wigner resonance shape is recovered:

$$\sigma_{\text{res}}(s) = \sigma_0 \frac{s\hat{\Gamma}_Z^2}{(s - \hat{M}_Z^2)^2 + \hat{M}_Z^2\hat{\Gamma}_Z^2} \quad (122)$$

Numerically one finds: $\hat{M}_Z - M_Z \simeq -34$ MeV, $\hat{\Gamma}_Z - \Gamma_Z \simeq -1$ MeV. σ_0 is not changed. \hat{M}_Z corresponds to the real part of the S -matrix pole of the Z -resonance [58].

From line-shape measurements one obtains the parameters M_Z , Γ_Z , σ_0 or the partial widths, respectively. M_Z is used as a precise input parameter, together with α and G_μ ; the width and partial widths allow comparisons with the predictions of the Standard Model.

The total Z width Γ_Z can be calculated essentially as the sum over the fermionic partial decay widths. Expressed in terms of the effective coupling constants, they read up to second

order in the fermion masses:

$$\Gamma_f = \Gamma_0 \left[|g_V^f|^2 + |g_A^f|^2 \left(1 - \frac{6m_f^2}{M_Z^2} \right) \right] \cdot \left(1 + Q_f^2 \frac{3\alpha}{4\pi} \right) + \Delta\Gamma_{\text{QCD}}^f \quad (123)$$

with

$$\Gamma_0 = N_C^f \frac{\sqrt{2}G_\mu M_Z^3}{12\pi}, \quad N_C^f = 1 \text{ (leptons)}, \quad = 3 \text{ (quarks)}.$$

The QCD correction for the light quarks with $m_q \simeq 0$ is given by

$$\Delta\Gamma_{\text{QCD}}^f = \Gamma_0 \left(|g_V^f|^2 + |g_A^f|^2 \right) \cdot K_{\text{QCD}} \quad (124)$$

with [59]

$$K_{\text{QCD}} = \frac{\alpha_s}{\pi} + 1.41 \left(\frac{\alpha_s}{\pi} \right)^2 - 12.8 \left(\frac{\alpha_s}{\pi} \right)^3 - \frac{Q_f^2}{4} \frac{\alpha\alpha_s}{\pi^2}. \quad (125)$$

For b quarks the QCD corrections are different, because of finite b mass terms and to top-quark-dependent 2-loop diagrams for the axial part:

$$\Delta\Gamma_{\text{QCD}}^b = \Delta\Gamma_{\text{QCD}}^d + \Gamma_0 \left[|g_V^b|^2 R_V + |g_A^b|^2 R_A \right]. \quad (126)$$

The coefficients in the perturbative expansions

$$\begin{aligned} R_V &= c_1^V \frac{\alpha_s}{\pi} + c_2^V \left(\frac{\alpha_s}{\pi} \right)^2 + c_3^V \left(\frac{\alpha_s}{\pi} \right)^3 + \dots, \\ R_A &= c_1^A \frac{\alpha_s}{\pi} + c_2^A \left(\frac{\alpha_s}{\pi} \right)^2 + \dots \end{aligned}$$

depending on m_b and m_t , are calculated up to third order in α_s , except for the m_b -dependent singlet terms, which are known to $O(\alpha_s^2)$ [60,61]. For a review of the QCD corrections to the Z width, see [62].

The partial decay rate into b -quarks, in particular the ratio $R_b = \Gamma_b/\Gamma_{\text{had}}$, is an observable of special sensitivity to the top quark mass. Therefore, beyond the pure QCD corrections, also the 2-loop contributions of the mixed QCD-electroweak type, are important. The QCD corrections were first derived for the leading term of $O(\alpha_s G_\mu m_t^2)$ [63] and were subsequently completed by the $O(\alpha_s)$ correction to the residual terms of $O(\alpha\alpha_s)$ [64-66]. In the same spirit, also the complete 2-loop $O(\alpha\alpha_s)$ to the partial widths into the light quarks have been obtained, beyond those that are already contained in the factorized expression (124) with the electroweak 1-loop couplings [67].

6. Standard Model and precision data

We now confront the Standard Model predictions for the set of precision observables with experimental data. The Z -boson observables form LEP 1 and SLC together with M_W and the top-quark mass from LEP 2 and the Tevatron, constitute the set of high-energy quantities entering a global precision analysis (see [68] for a recent review).

From low-energy experiments, the quantity $s_W^2 = M_W/M_Z$ can indirectly be measured in deep-inelastic neutrino-nucleon scattering. The result of the NuTeV collaboration [69] can be expressed as follows,

$$\begin{aligned} s_W^2 &= 0.2277 \pm 0.0013 \pm 0.0009 \\ &\quad -0.00022 \frac{m_t^2 - (175 \text{ GeV})^2}{(50 \text{ GeV})^2} \\ &\quad + 0.00032 \ln(M_H/150 \text{ GeV}). \end{aligned}$$

Global fits within the Standard Model to the electroweak precision data contain M_H as the only free parameter. Figure 4, showing the deviation of the individual quantities from the Standard Model best-fit values, points out the forward-backward asymmetry for b quarks and s_W^2 from deep-inelastic neutrino scattering as the largest deviations from the standard model value for the best fit.

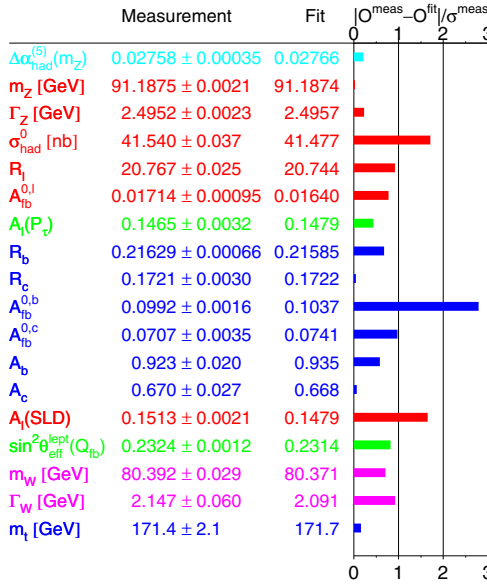


Figure 4. Experimental results and pulls from a standard model fit [68]. Pull = $\text{obs}(\text{exp}) - \text{obs}(\text{SM}) / (\text{exp.error})$.

The upper limit on the Higgs mass at the one-sided 95% C.L. is now $M_H < 166$ GeV, where the theoretical uncertainty is included (band in Figure 5). This bound is shifted to $M_H < 199$ GeV when the LEP-2 exclusion limit of 114 GeV is included. Thereby the hadronic vacuum polarization in Eq. (88) has been used (solid line in Figure 5). Improvements of $\Delta\alpha_{\text{had}}$ lead to a small shift in the central value; the 1σ upper bound on M_H is influenced only marginally. The reason is that, simultaneously with the shift in the central value to larger M_H , the error is reduced (see Figure 5).

As a central message, it can be concluded that the indirect determination of the Higgs mass range has shown that the Higgs boson is light, with its mass well below the non-perturbative regime (see section 8)

6.1. Muon anomalous magnetic moment

The anomalous magnetic moment of the muon,

$$a_\mu = \frac{g_\mu - 2}{2} \quad (127)$$

provides a precision test at low energies. The new experimental result of E 821 at Brookhaven National Laboratory [70] has reached a substantial improvement in accuracy. It shows a deviation from the Standard Model prediction by 2.7 [1.4] standard deviations depending on the evaluation of the hadronic vacuum polarization from data based on e^+e^- annihilation [hadronic τ decays together with isospin rotation], see [71].

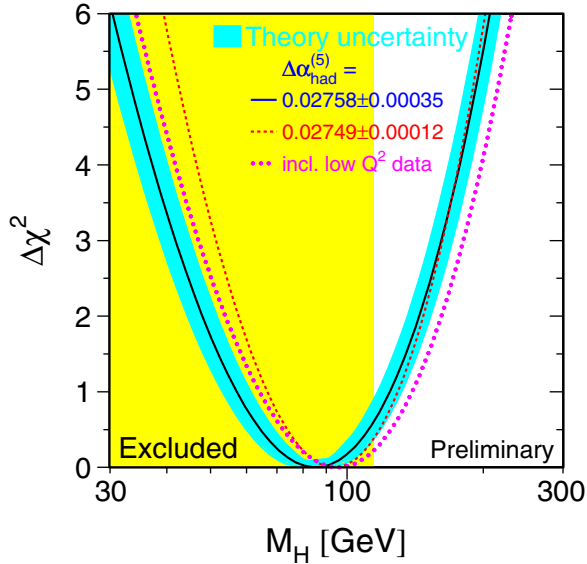


Figure 5. Higgs mass dependence of χ^2 in the global fit to precision data [68]. The shaded band displays the error from the theoretical uncertainties.

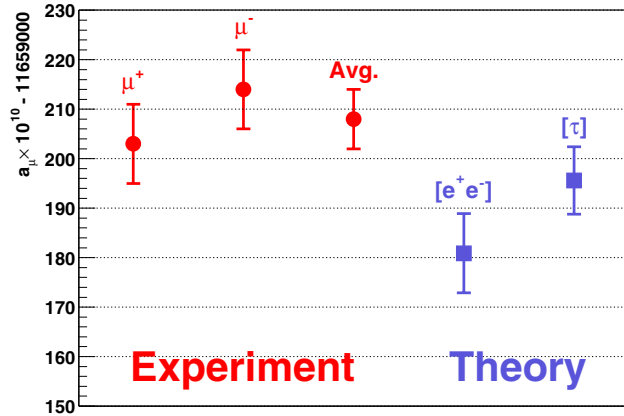


Figure 6. Anomalous g -factor of the muon, Standard Model prediction and experimental data.

7. The vector-boson self-interaction

The success of the Standard Model in the correct description of the electroweak precision observables is simultaneously an indirect confirmation of the Yang–Mills structure of the gauge boson self-interaction. For conclusive confirmations the direct experimental investigation is required. At LEP 2 (and higher energies), pair production of on-shell W bosons is studied experimentally, allowing tests of the trilinear vector boson self-couplings and precise M_W measurements. For LEP 2, an error of 33 MeV in M_W has been reached. Further improvements are being obtained from the Tevatron Run II with presently 59 MeV uncertainty, and in future from the LHC, with $\delta M_W \simeq 15$ MeV.

Pair production of W bosons in the Standard Model is described in Born approximation by the amplitude based on the Feynman graphs in Figure 7.

Besides the t -channel ν -exchange diagram, which involves only the W –fermion coupling,

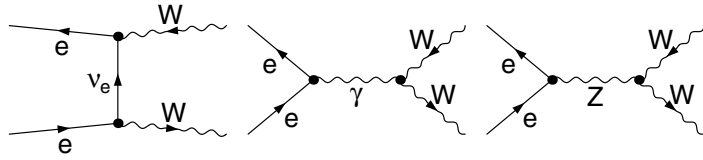


Figure 7. Feynman graphs for $e^+e^- \rightarrow W^+W^-$ in lowest order.

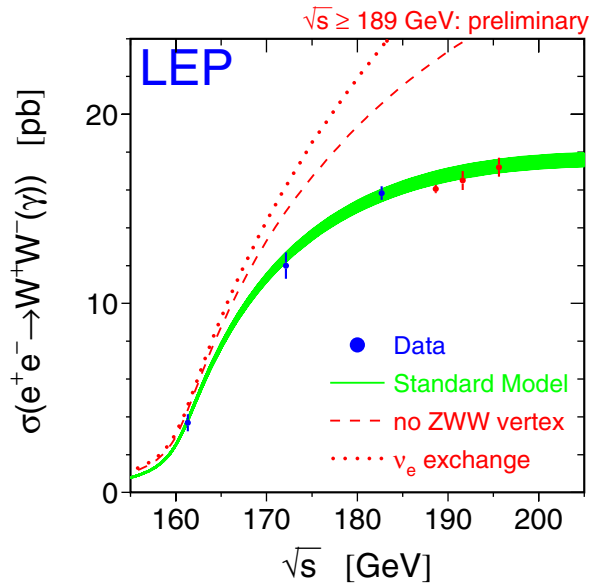


Figure 8. Cross-section for $e^+e^- \rightarrow W^+W^-$, measured at LEP, and the Standard Model prediction.

the s -channel diagrams contain the triple gauge interaction between the vector bosons. The gauge self-interactions of the vector bosons are essential for the high-energy behaviour of the production cross-section in accordance with the principle of unitarity. The self-interaction of the vector bosons is part of the Lagrangian (4); generalizing the triple couplings one finds, with the notation

$$F_{\mu\nu} = \partial_\mu A_\nu - \partial_\nu A_\mu$$

and $Z_{\mu\nu}$ and $W_{\mu\nu}^+$ analogously (replacing $A \rightarrow Z, W^+$):

$$\begin{aligned} \mathcal{L}_{WW\gamma/Z} = & e \left[(\partial_\mu W_\nu^+ - \partial_\nu W_\mu^+) W^{-\mu} A^\nu \right. \\ & + \kappa_\gamma W_\mu^+ W_\nu^- F^{\mu\nu} \\ & + \frac{\lambda_\gamma}{M_W^2} W_{\rho\mu}^+ W_\nu^{-\mu} F^{\rho\nu} + \text{h. c.} \left. \right] \\ & + e \cot \theta_W \left[(\partial_\mu W_\nu^+ - \partial_\nu W_\mu^+) W^{-\mu} Z^\nu \right. \\ & \left. + \kappa_Z W_\mu^+ W_\nu^- Z^{\mu\nu} \right] \end{aligned}$$

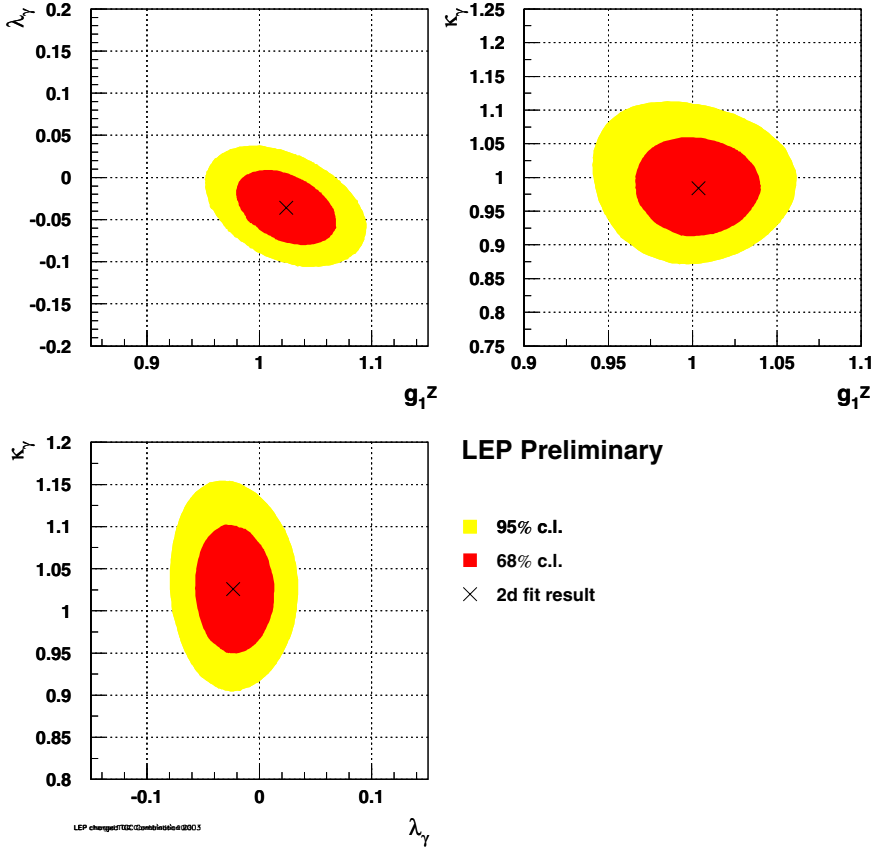


Figure 9. Bounds on anomalous triple-boson couplings from $e^+e^- \rightarrow W^+W^-$ measured at LEP.

$$+ \frac{\lambda_Z}{M_W^2} W_{\rho\mu}^+ W_{\nu}^{-\mu} Z^{\rho\nu} + \text{h. c.} \quad (128)$$

In the Standard Model the coefficients have the values, dictated by gauge invariance according to section 2.1,

$$\kappa_\gamma = \kappa_Z = 1, \quad \lambda_\gamma = \lambda_Z = 0. \quad (129)$$

Deviations from these values spoil the high-energy behaviour of the cross-sections and would be visible at energies sufficiently above the production threshold. Measurements of the cross section for $e^+e^- \rightarrow WW$ at LEP have confirmed the prediction of the Standard Model, as visualized in Figure 8 [68].

The non-observation of deviations from the Standard Model predictions can be converted into bounds on potential deviations of the trilinear coupling constants from their Standard Model values (denoted as anomalous couplings), which might be assigned to new physics beyond the minimal model. Those bounds are displayed in Figure 9 [68].

Experimentally, WW final states are identified through their fermionic decay products. In view of the experimental precision, Standard Model calculations for the process $e^+e^- \rightarrow W^+W^- \rightarrow 4f$ and the corresponding 4-fermion background processes are mandatory at the accuracy level of at least 1%. This requires the understanding of the radiative corrections to the W boson production and decay processes, as well as a careful treatment of the finite-widths effects. The systematic treatment of the complete radiative corrections is a task of enormous

complexity. For practical purposes, improved Born approximations have been in use for both resonating and non-resonating processes, dressed by initial-state QED corrections. Recently, a complete one-loop calculation has become available [72], decreasing the theoretical error below the per-cent level.

8. The standard Higgs sector

The minimal model with a single scalar doublet is the simplest way to implement the electroweak symmetry breaking. The experimental result that the ρ -parameter is very close to unity is a natural feature of models with doublets and singlets. The Higgs potential of the Standard Model, as given in Eq.(9), reads in the unitary gauge as follows:

$$\begin{aligned} V &= -\mu^2 H^2 + \frac{\mu^2}{v} H^3 + \frac{\mu^2}{4v^2} H^4 \\ &= -\frac{M_H^2}{2} H^2 + \frac{M_H^2}{2v} H^3 + \frac{M_H^2}{8v^2} H^4. \end{aligned} \quad (130)$$

The vacuum expectation value

$$v = (\sqrt{2}G_\mu)^{-1/2} \quad (131)$$

is fixed by the gauge sector. Thus, in the Standard Model the mass M_H of the Higgs boson appears as the only additional parameter beyond the vector boson and fermion masses. M_H cannot be predicted but has to be taken from experiment. The present lower limit (95% C.L.) from the search at LEP [71] is 114 GeV. Indirect determinations of M_H from precision data have already been discussed in section 6. The indirect mass bounds react sensitively to small changes in the input data, which is a consequence of the logarithmic dependence of electroweak precision observables. As a general feature, it appears that the data prefer a light Higgs boson.

There are also theoretical constraints on the Higgs mass from vacuum stability and absence of a Landau pole [73-75], and from lattice calculations [76]. Explicit perturbative calculations of the decay width for $H \rightarrow W^+W^-$, ZZ in the large- M_H limit in 2-loop order [78] have shown that the 2-loop contribution exceeds the 1-loop term in size (same sign) for $M_H > 930$ GeV (Figure 10 [81]). This result is confirmed by the calculation of the next-to-leading order correction in the $1/N$ expansion, where the Higgs sector is treated as an $O(N)$ symmetric σ -model [79]. A similar increase of the 2-loop perturbative contribution with M_H is observed for the fermionic decay [80] $H \rightarrow f\bar{f}$, but with opposite sign leading to a cancellation of the one-loop correction for $M_H \simeq 1100$ GeV (Figure 10). The lattice result [77] for the bosonic Higgs decay in Figure 10 for $M_H = 727$ GeV is not far from the perturbative 2-loop result. The difference may at least partially be interpreted as missing higher-order terms.

The behaviour of the quartic Higgs self-coupling λ , as a function of a rising energy scale μ , follows from the renormalization group equation with the β -function dominated by the contributions from λ and the top quark Yukawa coupling g_t ,

$$\frac{d\lambda}{dt} = \frac{1}{16\pi^2} (12\lambda^2 + 6\lambda g_t^2 - 3g_t^4 + \dots), \quad t = \log \frac{\mu^2}{v^2}. \quad (132)$$

In order to avoid unphysical negative quartic couplings from the negative top quark contribution, a lower bound on the Higgs mass is derived. The requirement that the Higgs coupling remains finite and positive up to a scale Λ yields constraints on the Higgs mass M_H , which have been evaluated at the 2-loop level [74,75]. These bounds on M_H are shown in Figure 11 [75] as a function of the cut-off scale Λ up to which the standard Higgs sector can be extrapolated. The allowed region is the area between the lower and the upper curves. The bands indicate the theoretical uncertainties associated with the solution of the renormalization group equations [75]. It is interesting to note that the indirect determination of the Higgs mass range from

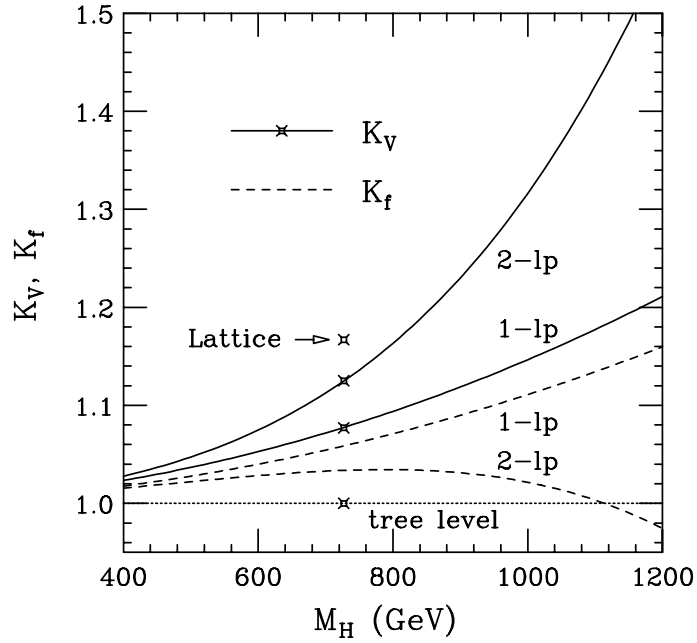


Figure 10. Correction factors for the Higgs decay widths $H \rightarrow VV$ ($V = W, Z$) and $H \rightarrow f\bar{f}$ in 1- and 2-loop order.

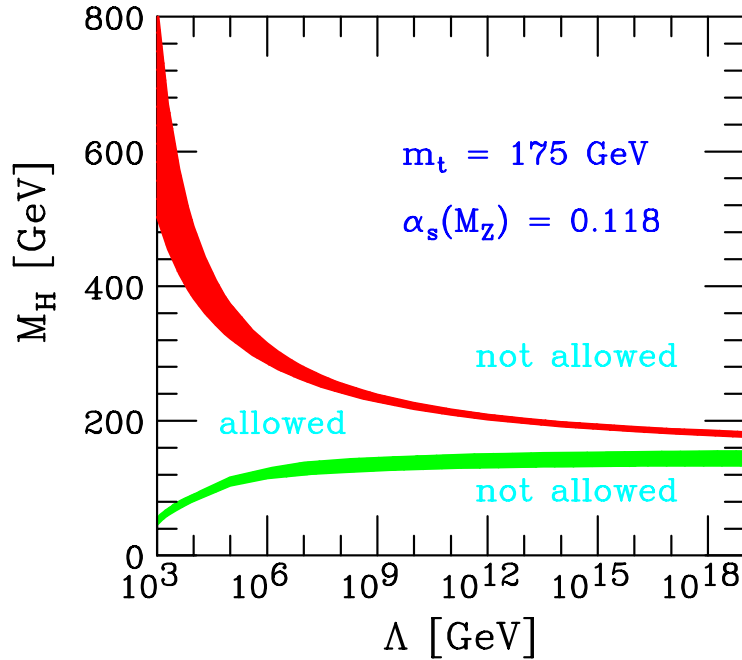


Figure 11. Theoretical limits on the Higgs boson mass from the absence of a Landau pole and from vacuum stability.

electroweak precision data via radiative corrections is compatible with a value of M_H where Λ can be extended up to the Planck scale.

9. The minimal supersymmetric standard model (MSSM)

9.1. The light Higgs boson of the MSSM

The existence of a light Higgs boson, in the mass range below 135 GeV, is a definite prediction of the MSSM. In contrast to the standard model, its mass m_h is not a free parameter but depends on the other parameters of the model. The prediction for m_h , therefore, is a crucial theoretical tool to probe the MSSM parameter space. From the experimental side, the Higgs mass can be measured with high accuracy: 100 MeV at the LHC, and 50 MeV at a Linear e^+e^- Collider. m_h is, hence, another precision observable in the MSSM. The precise theoretical value is very sensitive to higher-order effects (see the discussion in [82] and further references given therein). An illustrative example for the influence of higher-order contributions is shown in Figure 12, based on FEYNHIGGS [83]

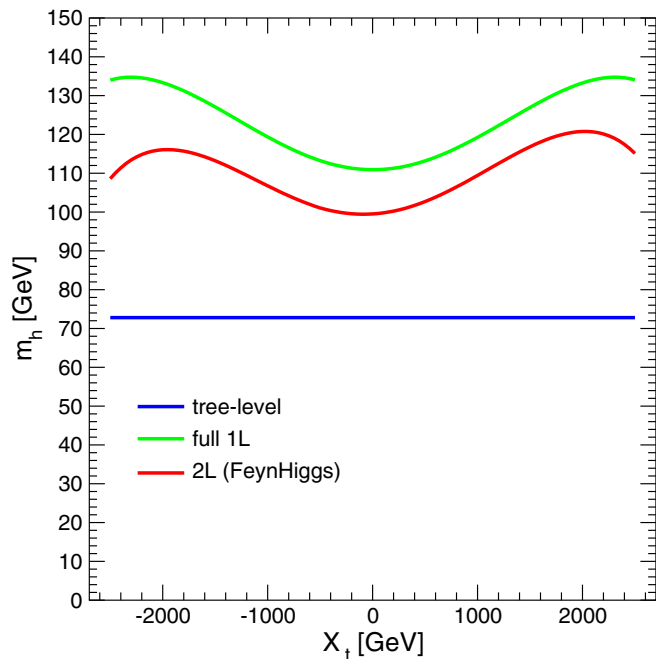


Figure 12. The lightest Higgs-boson mass in the MSSM, in various orders of perturbation theory [83]. SUSY parameters: $\tan\beta = 3$, $M_{\tilde{Q}} = M_2 = \mu = M_A = 1$ TeV, $m_{\tilde{g}} = 800$ GeV. X_t is the non-diagonal entry in the top-squark mass matrix.

9.2. The MSSM and precision data

Among the extensions of the standard model, the MSSM is the theoretically favoured scenario as the most predictive framework beyond the standard model. A definite prediction of the MSSM is the existence of a light Higgs boson with mass below ~ 135 GeV [82]. The detection of a light Higgs boson could be a significant hint for supersymmetry.

The structure of the MSSM as a renormalizable quantum field theory allows a similarly complete calculation of the electroweak precision observables as in the standard model in terms of one Higgs mass (usually taken as the CP -odd ‘pseudoscalar’ mass M_A) and $\tan\beta = v_2/v_1$, together with the set of SUSY soft-breaking parameters fixing the chargino/neutralino and scalar fermion sectors (see [84] for a recent review). The general discussion of renormalization of the MSSM to all orders with implications on the structure of the counter terms is given in [85].

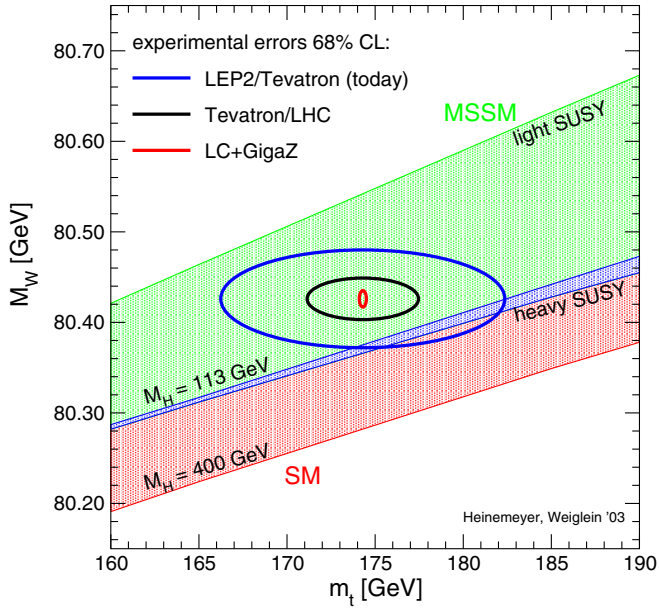


Figure 13. The W mass range in the standard model (lower band) and in the MSSM (upper band). Bounds are from the non-observation of Higgs bosons and SUSY particles.

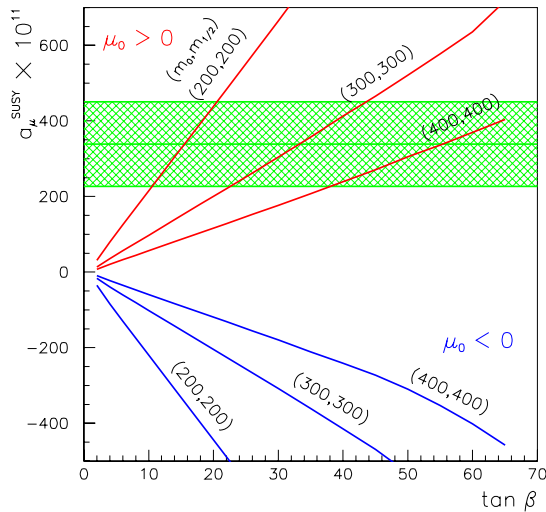


Figure 14. Supersymmetric contribution to a_μ [93]. The deviation of the measured value from the Standard Model prediction is indicated by the horizontal band.

Complete 1-loop calculations are available for Δr [86] and for the Z boson observables [87], with recent 2-loop improvements [88].

A possible mass splitting between \tilde{b}_L and \tilde{t}_L yields a contribution to the ρ -parameter of the same sign as the standard top term. As a universal loop contribution, it enters the quantity Δr and the Z boson couplings and is thus significantly constrained by the data. The 2-loop α_s -corrections have been computed in [89], and the electroweak 2-loop contribution from the

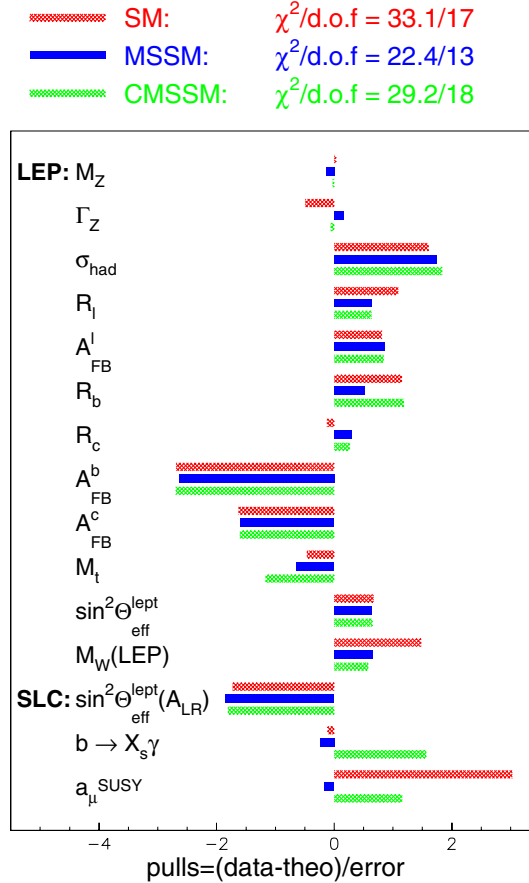


Figure 15. Best fits in the SM and in the MSSM, normalized to the data [93]. Error bars are those from data.

Yukawa couplings in [90].

As an example, Figure 13 displays the range of predictions for M_W in the minimal model and in the MSSM, together with the present experimental errors and the expectations for the future colliders LHC and LC. As can be seen, the MSSM prediction is in better agreement with the present data, although not conclusive as yet. Future increase in the experimental accuracy, however, will become decisive for the separation between the models.

Especially for the muonic $g - 2$, the MSSM can significantly improve the agreement between theory and experiment: relatively light scalar muons, muon-sneutrinos and charginos/neutralinos, together with a large value of $\tan \beta$ can provide a positive contribution Δa_μ which can entirely explain the difference $a_\mu^{\text{exp}} - a_\mu^{\text{SM}}$ [91]. Figure 14 illustrates the MSSM contribution for universal SUSY scalar mass parameters m_0 and spin-1/2 mass parameters $m_{1/2}$.

The MSSM yields a comprehensive description of the precision data, in a similar way as the Standard Model does. Global fits, varying the MSSM parameters, are available [92] to all electroweak precision data. They have been updated [93], showing that the description within the MSSM is slightly better than in the standard model. This is mainly due to the improved agreement for a_μ (see Figure 15). The situation for A_{FB}^b , however, remains unaltered.

As far as the deviation of the NuTeV result (127) from the Standard Model prediction is concerned, the MSSM fails to improve the situation [94].

10. Conclusions

The electroweak Standard Model has developed into the quantum field theory of the electromagnetic and weak interactions. The experimental data for testing the electroweak theory have achieved an impressive accuracy. For the interpretation of the precision experiments radiative corrections, or quantum effects, play a crucial role. The calculation of radiative corrections is theoretically well established, and many contributions have become available over the past years to improve and stabilize the Standard Model predictions. After taking the measured Z mass, besides α and G_μ , for completion of the input, each other precision observable provides a test of the electroweak theory. The theoretical predictions of the Standard Model depend on the mass of the top quark and of the as yet experimentally unknown Higgs boson through the virtual presence of these particles in the loops. As a consequence, precision data can be used to pin down the allowed range of the mass parameters.

The comparison of the theoretical predictions with experimental data has confirmed the validity of the Standard Model in a convincing way:

- the description of the data is of high quality, with small deviations which might be considered as normal;
- the quantum effects of the Standard Model have been established at the level of several σ ;
- direct and indirect determinations of the top-quark mass are compatible with each other;
- the Higgs-boson mass is meanwhile also being constrained within the perturbative mass regime with the possibility that the Standard Model may be extrapolated up to energies around the Planck scale.

In spite of this success, the conceptual situation with the Standard Model is unsatisfactory for quite a few deficiencies:

- the smallness of the electroweak scale $v \sim 246 \text{ GeV} \ll M_{\text{Pl}}$ (the so-called hierarchy problem);
- the large number of free parameters (gauge couplings, vacuum expectation value, M_H , fermion masses, CKM matrix elements), which are not predicted but have to be taken from experiments;
- the pattern that occurs in the arrangement of the fermion masses;
- the missing way to connect to gravity.

Supersymmetry may help to provide at least part of the answers, such as stabilizing the electroweak scale and opening the possibility to further unification of the fundamental forces within GUT scenarios. The MSSM, mainly theoretically advocated, is competitive to the standard model in describing the data with improvements in specific observables, although not conclusive. Since the MSSM predicts the existence of a light Higgs boson, the detection of a Higgs particle could be an indication of supersymmetry. It is therefore highly important to study the different features of such a Higgs boson in the various models at a level of high precision. Moreover, precision studies of supersymmetric particles will become necessary for revealing the mechanism of SUSY breaking and will require a proper inclusion of higher-order effects as well.

References

- [1] S.L. Glashow, *Nucl. Phys. B* **22**, 579 (1961);
S. Weinberg, *Phys. Rev. Lett.* **19**, 1264 (1967);
A. Salam, in: *Proceedings of the 8th Nobel Symposium*, p. 367, ed. N. Svartholm, Almqvist and Wiksell, Stockholm 1968
- [2] S.L. Glashow, I. Iliopoulos, L. Maiani, *Phys. Rev. D* **2**, 1285 (1970);
- [3] N. Cabibbo, *Phys. Rev. Lett.* **10**, 531 (1963);
M. Kobayashi, K. Maskawa, *Prog. Theor. Phys.* **49**, 652 (1973)
- [4] G. 't Hooft, *Nucl. Phys. B* **33**, 173 (1971); *Nucl. Phys. B* **35**, 167 (1971)
- [5] L.D. Faddeev, V.N. Popov, *Phys. Lett. B* **25**, 29 (1967)
- [6] G. Passarino, M. Veltman, *Nucl. Phys. B* **160**, 151 (1979)
- [7] G. 't Hooft, M. Veltman, *Nucl. Phys. B* **135**, 365 (1979)
- [8] C. Bollini, J. Giambiagi *Nuovo Cim. B* **12**, 20 (1972);

J. Ashmore, *Nuovo Cim. Lett.* **4**, 289 (1972);
 G. 't Hooft, M. Veltman, *Nucl. Phys. B* **44**, 189 (1972)

[9] P. Breitenlohner, D. Maison, *Comm. Math. Phys.* **52**, 11, 39, 55 (1977)

[10] M. Böhm, W. Hollik, H. Spiesberger, *Fortschr. Phys.* **34**, 687 (1986)

[11] D. Ross, M. Veltman, *Nucl. Phys. B* **95**, 135 (1975);
 M. Veltman, *Nucl. Phys. B* **123**, 89 (1977);
 D. Ross, M. Veltman, *Nucl. Phys. B* **95**, 135 (1975);
 M.S. Chanowitz, M.A. Furman, I. Hinchliffe, *Phys. Lett. B* **78**, 285 (1978)

[12] D.A. Ross, J.C. Taylor, *Nucl. Phys. B* **51**, 25 (1973)

[13] M. Consoli, *Nucl. Phys. B* **160**, 208 (1979)

[14] A. Sirlin, *Phys. Rev. D* **22**, 971 (1980);
 W. J. Marciano, A. Sirlin, *Phys. Rev. D* **22**, 2695 (1980);
 A. Sirlin, W. J. Marciano, *Nucl. Phys. B* **189**, 442 (1981)

[15] D.Yu. Bardin, P.Ch. Christova, O.M. Fedorenko, *Nucl. Phys. B* **175**, 435 (1980) and B **197**, 1 (1982);
 D.Yu. Bardin, M.S. Bilenky, G.V. Mithselmakher, T. Riemann, M. Sachwitz, *Z. Phys. C* **44**, 493 (1989)

[16] J. Fleischer, F. Jegerlehner, *Phys. Rev. D* **23**, 2001 (1981)

[17] K.I. Aoki, Z. Hioki, R. Kawabe, M. Komuma,
 T. Muta, *Suppl. Prog. Theor. Phys.* **73**, 1 (1982);
 Z. Hioki, *Phys. Rev. Lett.* **65**, 683 (1990), E: *ibidem* **65**, 1692 (1990); *Z. Phys. C* **49**, 287 (1991)

[18] M. Consoli, S. LoPresti, L. Maiani, *Nucl. Phys. B* **223**, 474 (1983)

[19] D.Yu. Bardin, M.S. Bilenky, G.V. Mithselmakher, T. Riemann, M. Sachwitz, *Z. Phys. C* **44**, 493 (1989)

[20] W. Hollik, *Fortschr. Phys.* **38**, 165 (1990)

[21] M. Consoli, W. Hollik, F. Jegerlehner, in: *Z Physics at LEP 1*, eds. G. Altarelli, R. Kleiss and C. Verzegnassi, CERN 89-08 (1989)

[22] G. Passarino, R. Pittau, *Phys. Lett. B* **228**, 89 (1989);
 V.A. Novikov, L.B. Okun, M.I. Vysotsky, *Nucl. Phys. B* **397**, 35 (1993)

[23] M. Veltman, *Phys. Lett. B* **91**, 95 (1980);
 M. Green, M. Veltman, *Nucl. Phys. B* **169**, 137 (1980), E: *Nucl. Phys. B* **175**, 547 (1980);
 F. Antonelli, M. Consoli, G. Corbo, *Phys. Lett. B* **91**, 90 (1980);
 F. Antonelli, M. Consoli, G. Corbo, O. Pellegrino, *Nucl. Phys. B* **183**, 195 (1981)

[24] G. Passarino, M. Veltman, *Phys. Lett. B* **237**, 537 (1990)

[25] W.J. Marciano, A. Sirlin, *Phys. Rev. Lett.* **46**, 163 (1981);
 A. Sirlin, *Phys. Lett. B* **232**, 123 (1989)

[26] G. Degrassi, S. Fanchiotti, A. Sirlin, *Nucl. Phys. B* **351**, 49 (1991)

[27] G. Degrassi, A. Sirlin, *Nucl. Phys. B* **352**, 342 (1991)

[28] J.C. Ward, *Phys. Rev.* **78**, 1824 (1950)

[29] R.E. Behrends, R.J. Finkelstein, A. Sirlin, *Phys. Rev.* **101**, 866 (1956);
 T. Kinoshita, A. Sirlin, *Phys. Rev.* **113**, 1652 (1959)

[30] T. van Ritbergen, R. Stuart, *Phys. Lett. B* **437**, 201 (1998), *Phys. Rev. Lett.* **82**, 488 (1999)

[31] G. Källén, A. Sabry, *K. Dan. Vidensk. Selsk. Mat.-Fys. Medd.* **29** (1955) No. 17

[32] M. Steinhauser, *Phys. Lett. B* **429**, 158 (1998)

[33] F. Jegerlehner, hep-ph/0310234 and hep-/p/0312372

[34] H. Burkhardt, B. Pietrzyk, *Phys. Rev. D* **72**, 057501 (2005)

[35] M. Veltman, *Acta Phys. Polon. B* **8**, 475 (1977)

[36] W.J. Marciano, *Phys. Rev. D* **20**, 274 (1979)

[37] M. Consoli, W. Hollik, F. Jegerlehner, *Phys. Lett. B* **227**, 167 (1989)

[38] J.J. van der Bij, F. Hoogeveen, *Nucl. Phys. B* **283**, 477 (1987)

[39] R. Barbieri, M. Beccaria, P. Ciafaloni, G. Curci, A. Vicere, *Phys. Lett. B* **288**, 95 (1992); *Nucl. Phys. B* **409**, 105 (1993);
 J. Fleischer, F. Jegerlehner, O.V. Tarasov, *Phys. Lett. B* **319**, 249 (1993)

[40] J.J. van der Bij, M. Veltman, *Nucl. Phys. B* **231**, 205 (1985)

[41] J.J. van der Bij, K.G. Chetyrkin, M. Faisst, G. Jikia, T. Seidensticker, *Phys. Lett. B* **498**, 156 (2001);
 M. Faisst, J.H. Kühn, T. Seidensticker, O. Veretin, *Nucl. Phys. B* **665**, 649 (2003)

[42] R. Boughezal, J.B. Tausk, J.J. van der Bij, *Nucl. Phys. B* **713**, 278 (2005)

[43] A. Djouadi, C. Verzegnassi, *Phys. Lett. B* **195**, 265 (1987)

[44] L. Avdeev, J. Fleischer, S. M. Mikhailov, O. Tarasov, *Phys. Lett. B* **336**, 560 (1994); E: *Phys. Lett. B* **349**, 597 (1995);
 K.G. Chetyrkin, J.H. Kühn, M. Steinhauser, *Phys. Lett. B* **351**, 331 (1995)

[45] Y. Schroder, M. Steinhauser, *Phys. Lett. B* **622**, 124 (2005);

K.G. Chetyrkin, M. Faisst, J.H. Kühn, P. Maierhofer, C. Sturm, hep-ph/0605201;
 R. Boughezal, M. Czakon, hep-ph/0606232

[46] A. Djouadi, *Nuovo Cim. A* **100**, 357 (1988);
 D. Yu. Bardin, A.V. Chizhov, Dubna preprint E2-89-525 (1989);
 B.A. Kniehl, *Nucl. Phys. B* **347**, 86 (1990);
 F. Halzen, B.A. Kniehl, *Nucl. Phys. B* **353**, 567 (1991) 567;
 A. Djouadi, P. Gambino, *Phys. Rev. D* **49**, 3499 (1994)

[47] B.A. Kniehl, J.H. Kühn, R.G. Stuart, *Phys. Lett. B* **214**, 621 (1988);
 B.A. Kniehl, A. Sirlin, *Nucl. Phys. B* **371**, 141 (1992); *Phys. Rev. D* **47**, 883 (1993);
 S. Fanchiotti, B.A. Kniehl, A. Sirlin, *Phys. Rev. D* **48**, 307 (1993)

[48] K. Chetyrkin, J.H. Kühn, M. Steinhauser, *Phys. Rev. Lett.* **75**, 3394 (1995)

[49] A. Freitas, W. Hollik, W. Walter, G. Weiglein, *Phys. Lett. B* **495**, 338 (2000); *Nucl. Phys. B* **632**, 189 (2002);
 M. Awramik, M. Czakon, *Phys. Lett. B* **568**, 48 (2003)

[50] M. Awramik, M. Czakon, *Phys. Rev. Lett.* **89**, 241801 (2002)

[51] A. Onishchenko, O. Veretin, *Phys. Lett. B* **551**, 111 (2003);
 M. Awramik, M. Czakon, A. Onishchenko, O. Veretin, *Phys. Rev. D* **68**, 053004 (2003)

[52] D. Bardin et al., hep-ph/9709229, in: *Reports of the Working Group on Precision Calculations for the Z Resonance*, p. 7, CERN 95-03 (1995), eds. D. Bardin, W. Hollik, G. Passarino

[53] A.A. Akhundov, D.Yu. Bardin, T. Riemann, *Nucl. Phys. B* **276**, 1 (1986);
 W. Beenakker, W. Hollik, *Z. Phys. C* **40**, 141 (1988);
 J. Bernabeu, A. Pich, A. Santamaria, *Phys. Lett. B* **200**, 569 (1988)

[54] A. Denner, W. Hollik, B. Lampe, *Z. Phys. C* **60**, 193 (1993)

[55] M. Awramik, M. Czakon, A. Freitas, G. Weiglein, *Phys. Rev. Lett.* **93**, (2004) and *Nucl. Phys. B Proc. Suppl.* **135**, 119 (2004);
 W. Hollik, U. Meier, S. Uccirati, *Nucl. Phys. B* **731**, 213 (2005) and *Phys. Lett. B* **632**, 680 (2006);
 M. Awramik, M. Czakon, A. Freitas, hep-ph/0605339, hep-ph/0608099.

[56] G. Burgers, F.A. Berends, W. Hollik, W.L. van Neerven, *Phys. Lett. B* **203**, 177 (1988)

[57] D. Yu. Bardin, A. Leike, T. Riemann, M. Sachwitz, *Phys. Lett. B* **206**, 539 (1988)

[58] G. Valencia, S. Willenbrock, *Phys. Lett. B* **259**, 373 (1991);
 R.G. Stuart, *Phys. Lett. B* **272**, 353 (1991) 353;
 A. Sirlin, *Phys. Rev. Lett.* **67**, 2127 (1991); *Phys. Lett. B* **267**, 240 (1991)

[59] K.G. Chetyrkin, A.L. Kataev, F.V. Tkachov, *Phys. Lett. B* **85**, 277 (1979);
 M. Dine, J. Sapirstein, *Phys. Rev. Lett.* **43**, 668 (1979);
 W. Celmaster, R. Gonsalves, *Phys. Rev. Lett.* **44**, 560 (1980);
 S.G. Gorishny, A.L. Kataev, S.A. Larin, *Phys. Lett. B* **259**, 144 (1991);
 L.R. Surguladze, M.A. Samuel, *Phys. Rev. Lett.* **66**, 560 (1991);
 A. Kataev, *Phys. Lett. B* **287**, 209 (1992)

[60] K.G. Chetyrkin, J.H. Kühn, *Phys. Lett. B* **248**, 359 (1990) and *B* **406**, 102 (1997);
 K.G. Chetyrkin, J.H. Kühn, A. Kwiatkowski, *Phys. Lett. B* **282**, 221 (1992);
 K.G. Chetyrkin, A. Kwiatkowski, *Phys. Lett. B* **305**, 285 (1993) and *B* **319**, 307 (1993)

[61] B.A. Kniehl, J.H. Kühn, *Phys. Lett. B* **224**, 229 (1990); *Nucl. Phys. B* **329**, 547 (1990);
 K.G. Chetyrkin, J.H. Kühn, *Phys. Lett. B* **307**, 127 (1993);
 S. Larin, T. van Ritbergen, J.A.M. Vermaasen, *Phys. Lett. B* **320**, 159 (1994);
 K.G. Chetyrkin, O.V. Tarasov, *Phys. Lett. B* **327**, 114 (1994)

[62] K.G. Chetyrkin, J.H. Kühn, A. Kwiatkowski, in *Reports of the Working Group on Precision Calculations for the Z Resonance*, p. 175, CERN 95-03 (1995), eds. D. Bardin, W. Hollik, G. Passarino;
 K.G. Chetyrkin, J.H. Kühn, A. Kwiatkowski, *Phys. Rep.* **277**, 189 (1996)

[63] J. Fleischer, F. Jegerlehner, P. Raczka, O.V. Tarasov, *Phys. Lett. B* **293**, 437 (1992);
 G. Buchalla, A.J. Buras, *Nucl. Phys. B* **398**, 285 (1993);
 G. Degrassi, *Nucl. Phys. B* **407**, 271 (1993);
 K.G. Chetyrkin, A. Kwiatkowski, M. Steinhauser, *Mod. Phys. Lett. A* **8**, 2785 (1993)

[64] A. Kwiatkowski, M. Steinhauser, *Phys. Lett. B* **344**, 359 (1995);
 S. Peris, A. Santamaria, *Nucl. Phys. B* **445**, 252 (1995)

[65] R. Harlander, T. Seidensticker, M. Steinhauser, *Phys. Lett. B* **426**, 125 (1998)

[66] J. Fleischer, F. Jegerlehner, M. Tentyukov, O. Veretin, *Phys. Lett. B* **459**, 625 (1999)

[67] A. Czarnecki, J.H. Kühn, *Phys. Rev. Lett.* **77**, 3955 (1996); *E*: **80**, 893 (1998)

[68] The LEP Collaborations ALEPH, DELPHI, L3, OPAL, the LEP Electroweak Working Group and the SLD Heavy Flavor and Electroweak Groups, *Phys. Rep.* **427**, 257 (2006);
 D. Wood, ICHEP 2006, Moscow 2006

[69] NuTev Collaboration, T. Bolton, in: *Proceedings of the XXIX International Conference on High Energy Physics*, Vancouver 1998, eds. A. Astbury, D. Axen, J. Robinson, World Scientific, Singapore 1999

[70] H.N. Brown et al., *Phys. Rev. Lett.* **86**, 2227 (2001); G.W. Bennett et al., *Phys. Rev. Lett.* **89**, 101804 (2002) and **92**, 161802 (2004)

[71] Particle data Group, W.M. Yao et al., *J. Phys. G* **33**, 1 (2006)

[72] A. Denner, S. Dittmaier, M. Roth, L.H. Wieders, *Phys. Lett. B* **612**, 223 (2005) and *Nucl. Phys. B* **724**, 247 (2005)

[73] L. Maiani, G. Parisi, R. Petronzio, *Nucl. Phys. B* **136**, 115 (1979);
N. Cabibbo, L. Maiani, G. Parisi, R. Petronzio, *Nucl. Phys. B* **158**, 259 (1979);
R. Dashen, H. Neuberger, *Phys. Rev. Lett.* **50**, 1897 (1983);
D.J.E. Callaway, *Nucl. Phys. B* **233**, 189;
M.A. Beg, C. Panagiotakopoulos, A. Sirlin, *Phys. Rev. Lett.* **52**, 883 (1984);
M. Lindner, *Z. Phys. C* **31**, 295 (1986)

[74] M. Lindner, M. Sher, H. Zaglauer, *Phys. Lett. B* **228**, 139 (1989);
G. Altarelli, G. Isidori, *Phys. Lett. B* **337**, 141 (1994);
J.A. Casas, J.R. Espinosa, M. Quiros, *Phys. Lett. B* **342**, 171 (1995) and **382**, 374 (1996);

[75] T. Hambye, K. Riesselmann, *Phys. Rev. D* **55**, 7255 (1997)

[76] Kuti et al., *Phys. Rev. Lett.* **61**, 678 (1988);
P. Hasenfratz et al., *Nucl. Phys. B* **317**, 81 (1989);
M. Lüscher, P. Weisz, *Nucl. Phys. B* **318**, 705 (1989);
M. Göckeler, H. Kastrup, T. Neuhaus, F. Zimmermann, *Nucl. Phys. B* **404**, 517 (1993)

[77] M. Göckeler, H. Kastrup, J. Westphalen, F. Zimmermann, *Nucl. Phys. B* **425**, 413 (1994)

[78] A. Ghinculov, *Nucl. Phys. B* **455**, 21 (1995);
A. Frink, B. Kniehl, K. Riesselmann, *Phys. Rev. D* **54**, 4548 (1996)

[79] T. Binoth, A. Ghinculov, J.J. van der Bij, *Phys. Rev. D* **57**, 1487 (1998); *Phys. Lett. B* **417**, 343 (1998)

[80] L. Durand, B.A. Kniehl, K. Riesselmann, *Phys. Rev. Lett.* **72**, 2534 (1994); E: *ibidem B* **74**, 1699 (1995);
A. Ghinculov, *Phys. Lett. B* **337**, 137 (1994); E: *ibidem B* **346**, 426 (1995);
V. Borodulin, G. Jikia, *Phys. Lett. B* **391**, 434 (1997)

[81] K. Riesselmann, hep-ph/9711456

[82] G. Degrassi, S. Heinemeyer, W. Hollik, P. Slavich, G. Weiglein, *Eur. Phys. J. C* **28**, 133 (2003)

[83] S. Heinemeyer, W. Hollik, G. Weiglein, *Comp. Phys. Comm.* **124**, 76 (2000). The updated version of *FeynHiggs* is available at <http://www.feynhiggs.de>

[84] S. Heinemeyer, W. Hollik, G. Weiglein, *Phys. Rep.* **425**, 265 (2006)

[85] W. Hollik, E. Kraus, M. Roth, C. Rupp, K. Sibold, D. Stöckinger, *Nucl. Phys. B* **639**, 3 (2002)

[86] P. Chankowski, A. Dabelstein, W. Hollik, W. Möslé, S. Pokorski, J. Rosiek, *Nucl. Phys. B* **417**, 101 (1994);
D. Garcia, J. Solà, *Mod. Phys. Lett. A* **9**, 211 (1994)

[87] D. Garcia, R. Jiménez, J. Solà, *Phys. Lett. B* **347**, 309 and 321 (1995); D. Garcia, J. Solà, *Phys. Lett. B* **357**, 349 (1995); A. Dabelstein, W. Hollik, W. Möslé, in *Perspectives for Electroweak Interactions in e^+e^- Collisions*, Ringberg Castle 1995, ed. B.A. Kniehl, World Scientific 1995 (p. 345); P. Chankowski, S. Pokorski, *Nucl. Phys. B* **475**, 3 (1996); J. Bagger, K. Matchev, D. Pierce, R. Zhang, *Nucl. Phys. B* **491**, 3 (1997)

[88] S. Heinemeyer, W. Hollik, D. Stöckinger, A. Weber, G. Weiglein, *JHEP* **0608**, 052 (2006)

[89] A. Djouadi, P. Gambino, S. Heinemeyer, W. Hollik, C. Jünger, G. Weiglein, *Phys. Rev. Lett.* **78**, 3626 (1997) and *Phys. Rev. D* **57**, 4179 (1998)

[90] S. Heinemeyer, G. Weiglein, *JHEP* **0210**, 072 (2002) and hep-ph/0301062

[91] A. Czarnecki, W. Marciano, *Phys. Rev. D* **64**, 013014 (2001)

[92] W. de Boer, A. Dabelstein, W. Hollik, W. Möslé, U. Schwickerath, *Z. Phys. C* **75**, 627 (1997)

[93] W. de Boer, C. Sander, *Phys. Lett. B* **585**, 276 (2004)

[94] S. Davidson, S. Forte, P. Gambino, N. Rius, A. Strumia, *JHEP* **0202**, 037 (2002); A. Kurylov, M.J. Ramsey-Musolf, S. Su, *Nucl. Phys. B* **667**, 321 (2003)